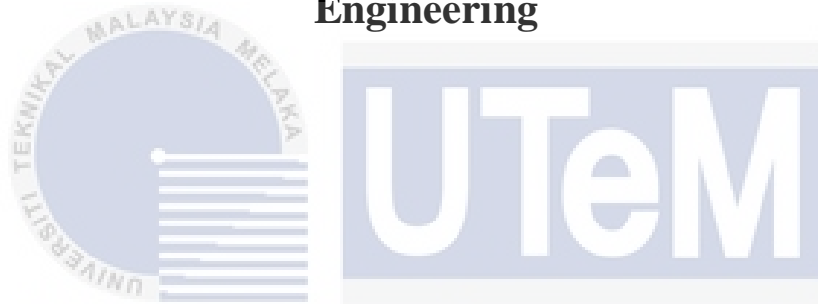




**Faculty of Electronics & Computer Technology and  
Engineering**



**MICROFIBRE DOUBLE LOOP RESONATOR FOR LIQUID SENSOR**

UNIVERSITI TEKNIKAL MALAYSIA MELAKA

**NUR ANISA BINTI SYAHRUNNIZAR**

**Bachelor of Electronics Engineering Technology (Telecommunications) with Honours**

**2024**

# **MICROFIBRE DOUBLE LOOP RESONATOR FOR LIQUID SENSOR**

**NUR ANISA BINTI SYAHRUNNIZAR**

**A project report submitted  
in partial fulfillment of the requirements for the degree of  
Bachelor of Electronics Engineering Technology (Telecommunications) with Honours**



**UNIVERSITI TEKNIKAL MALAYSIA MELAKA**

**2024**

**BORANG PENGESAHAN STATUS LAPORAN  
PROJEK SARJANA MUDA II**

Tajuk Projek : Microfibre Double Loop Resonator For Liquid Sensor

Sesi Pengajian : 2023/2024

Saya Nur Anisa Binti Syahrurnizar mengaku membenarkan laporan Projek Sarjana Muda ini disimpan di Perpustakaan dengan syarat-syarat kegunaan seperti berikut:

1. Laporan adalah hakmilik Universiti Teknikal Malaysia Melaka.
2. Perpustakaan dibenarkan membuat salinan untuk tujuan pengajian sahaja.
3. Perpustakaan dibenarkan membuat salinan laporan ini sebagai bahan pertukaran antara institusi pengajian tinggi.
4. Sila tandakan (✓):

**SULIT\***

(Mengandungi maklumat yang berdarjah keselamatan atau kepentingan Malaysia seperti yang termaktub di dalam AKTA RAHSIA RASMI 1972)

**TERHAD\***

(Mengandungi maklumat terhad yang telah ditentukan oleh organisasi/badan di mana penyelidikan dijalankan)

**TIDAK TERHAD**

Disahkan oleh:



(TANDATANGAN PENULIS)

Alamat Tetap: NO 175, Lorong Dahlia  
Taman Kamunting Jaya, 34600, Kamunting,  
Perak Darul Ridzuan



(COP DAN TANDATANGAN PENYELIA)

**DR. MD ASHADI BIN MD JOHARI**  
Pensyarah Kanan

Fakulti Teknologi Dan Kejuruteraan Elektronik Dan Komputer (FTKEK)  
Universiti Teknikal Malaysia Melaka (UTeM)

Tarikh: 17/12/2023

Tarikh: 20/01/2024

\*CATATAN: Jika laporan ini SULIT atau TERHAD, sila lampirkan surat daripada pihak berkuasa/organisasi berkenaan dengan menyatakan sekali tempoh laporan ini perlu dikelaskan sebagai SULIT atau TERHAD.

## DECLARATION

I declare that this project report entitled “Microfibre Double Loop Resonator For Liquid Sensor” is the result of my own research except as cited in the references. The project report has not been accepted for any degree and is not concurrently submitted in candidature of any other degree.

Signature

:



Student Name

:

Nur Anisa Binti Syahrannizar

Date

:

17/12/2023



اونيورسيتي تيكنيكل ماليزيا ملاك

UNIVERSITI TEKNIKAL MALAYSIA MELAKA

APPROVAL

I hereby declare that I have checked this project report and in my opinion, this project report is adequate in terms of scope and quality for the award of the degree of Bachelor of Electronics Engineering Technology (Telecommunications) with Honours.

Signature

:



Supervisor Name

:

DR. MD ASHADI BIN MD JOHARI

Date

:

20/01/2024

Signature



Co-Supervisor

:

Name (if any)

Date

:

UNIVERSITI TEKNIKAL MALAYSIA MELAKA



## DEDICATION

*To my beloved mother, Hayati binti Hasan, and father, Syahrunnizar bin Muhammad,  
To my kind lecturers and all my friends for their  
love, sacrifice, encouragement, and best wishes  
Along with all the hardworking and respected  
Supervisor Dr. Md Ashadi bin Md Johari*



## ABSTRACT

Reliable salt concentration readings are crucial in various aspects. Fibre optic sensors offer numerous advantages over electronic sensors, and extensive research has been conducted in recent years to explore their applications. This research project focuses on developing a fibre optic sensor specifically for salt concentration measurement. The project involves investigating the development of optical structures tailored for salt concentration determination and the exploration of novel materials suitable for this purpose. By utilizing a double-loop fibre structure, the fibre optic sensor is designed to detect and quantify salt concentration levels accurately. Understanding the relationship between salt concentration, air moisture, temperature, and humidity percentage is of great significance. By employing fibre optic technology, this research project aims to contribute to advancements in salt concentration sensing for the benefit of various aspects. The development of a reliable and accurate fibre optic sensor for salt concentration measurement holds the potential to enhance safety, improve treatment outcomes, and minimize the risks associated with improper salt concentration levels.

## ***ABSTRAK***

Bacaan konsentrasi garam yang dapat dipercayai adalah penting dalam pelbagai aspek. Penderia serat optik menawarkan pelbagai kelebihan berbanding penderia elektronik, dan penyelidikan yang meluas telah dijalankan dalam beberapa tahun kebelakangan ini untuk meneroka aplikasi mereka. Projek penyelidikan ini memberi tumpuan kepada pembangunan penderia serat optik khusus untuk pengukuran konsentrasi garam. Projek ini melibatkan penyiasatan pembangunan struktur optik yang disesuaikan untuk penentuan konsentrasi garam dan penjelajahan bahan baru yang sesuai untuk tujuan ini. Dengan menggunakan struktur serat optik dua litar, penderia serat optik direka untuk mengesan dan mengukur aras konsentrasi garam dengan tepat. Memahami hubungan antara konsentrasi garam, kelembapan udara, suhu, dan peratusan kelembapan adalah penting. Dengan menggunakan teknologi serat optik, projek penyelidikan ini bertujuan untuk menyumbang kepada kemajuan dalam pengesanan konsentrasi garam untuk kebaikan pelbagai aspek. Pembangunan penderia serat optik yang boleh dipercayai dan tepat untuk pengukuran konsentrasi garam mempunyai potensi untuk meningkatkan keselamatan, meningkatkan hasil rawatan, dan mengurangkan risiko yang berkaitan dengan aras konsentrasi garam yang tidak betul.

## ACKNOWLEDGEMENTS

First and foremost, I want thanks to Allah S.W.T for His blessing and guidance, which have given me the strength to finish the task successfully. I would like also to express my gratitude to my supervisor, Dr. Md Ashadi Bin Md Johari. Your guidance, expertise, and patience have shaped this project. I am grateful for your mentorship and the invaluable lessons I've learned under your supervision. Your dedication to excellence has been a constant source of inspiration. I am also indebted to Universiti Teknikal Malaysia Melaka (UTeM) for the financial support that enabled me to accomplish the project.

To my family, your enduring love and encouragement have been the driving force behind my academic journey. Thank you for standing by me and providing unwavering support. This achievement is as much yours as it is mine.

To friends, in the highs and lows of this academic endeavor, your friendship has been a source of strength and laughter. Thank you for being a sounding board, a motivator, and a true friend. Your support has made this journey memorable.

Last but not least, I want to thank me for believing in me, I want to thank me for doing all this hard work, I want to thank me for having no days off, I want to thank me for never quitting, I want to thank me for always being a giver and trying to give more than I receive.

## TABLE OF CONTENTS

	<b>PAGE</b>
<b>DECLARATION</b>	
<b>APPROVAL</b>	
<b>DEDICATIONS</b>	
<b>ABSTRACT</b>	<b>i</b>
<b>ABSTRAK</b>	<b>ii</b>
<b>ACKNOWLEDGEMENTS</b>	<b>iii</b>
<b>TABLE OF CONTENTS</b>	<b>iv</b>
<b>LIST OF TABLES</b>	<b>vii</b>
<b>LIST OF FIGURES</b>	<b>ix</b>
<b>LIST OF SYMBOLS</b>	<b>xii</b>
<b>LIST OF ABBREVIATIONS</b>	<b>xiii</b>
<b>LIST OF APPENDICES</b>	<b>xiv</b>
<b>CHAPTER 1 INTRODUCTION</b>	<b>1</b>
1.1 Background	1
1.2 Problem Statement	2
1.3 Project Objective	2
1.4 Scope of Project	3
<b>CHAPTER 2 LITERATURE REVIEW</b>	<b>4</b>
2.1 Introduction	4
2.2 Fibre Optic	4
2.2.1 Single – Mode	5
2.2.2 Multimode	6
2.3 Propagation of Light Among a Fibre	6
2.3.1 Total Internal Reflection	7
2.3.2 Numerical Aperture	8
2.4 Various Size of Fibre Optic Sensor	9
2.4.1 High – Resolution Fibre Optic Sensor based on Coated Linearly Chirped Bragg Grating	10
2.4.2 Sagnac Interference	11
2.4.3 Plastic Optical Fibre based Level Sensor Design	12
2.4.4 Plastic Fibre Optic Sensor of Continuous Liquid Level Monitoring	13
2.4.4.1 Material and Method	13
2.4.4.2 Discussion	14

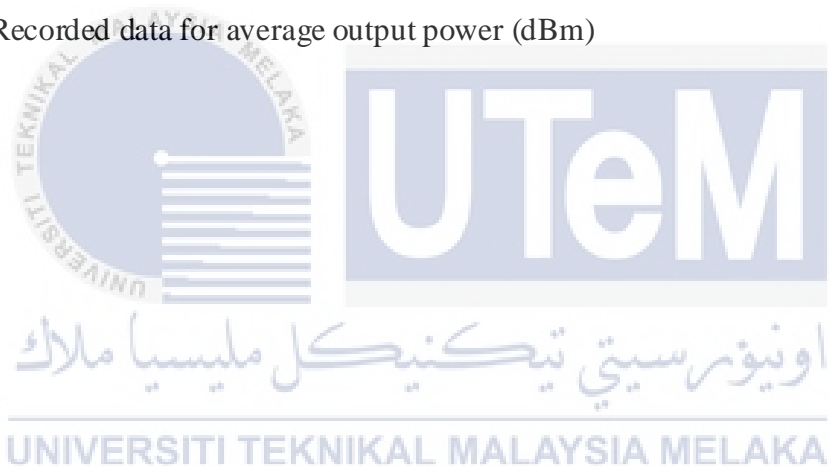
2.5	Tapared Optical Fibre	15
2.6	Sample of Table in Landscape orientation	16
2.7	Joumal Comparison from Previous Work Related to the Project	20
2.8	Summary	22
<b>CHAPTER 3 METHODOLOGY</b>		<b>23</b>
3.1	Introduction	23
3.2	Project Flow	28
3.3	Setting up an Experiment with Fibre Optic Sensors	30
3.3.1	Stripping Process	30
3.3.2	Cleaning Process	31
3.3.3	Cleaving Process	31
3.3.4	Splicing process	32
3.3.5	Tapered process	33
3.3.6	Single Looping Procedure	33
3.3.7	Double Looping Procedure	34
3.3.8	Final Check on Fibre	34
3.3.9	Characterization Fibre Optic Loop Sensor	35
3.3.10	Connector Inspection	35
3.3.11	Insertion Loss Test	36
3.3.12	Reflectance or Return Loss Test	37
3.3.13	Polarization Mode Dispersion	38
3.3.14	Summary	40
<b>CHAPTER 4 RESULTS AND DISCUSSIONS</b>		<b>42</b>
4.1	Introduction	42
4.2	Size of Microfiber Optic Loop Sensor	42
4.3	Result and Analysis for Different Level of Salt Concentration	43
4.3.1	Result for Single Loop	43
4.3.1.1	0 ml Level Salt Concentration Tested on 1310nm and 1550nm Wavelength	44
4.3.1.2	5ml Level Salt Concentration Tested on 1310nm and 1550nm Wavelength	45
4.3.1.3	10ml Level Salt Concentration Tested on 1310nm and 1550nm Wavelength	46
4.3.1.4	15ml Level Salt Concentration Tested on 1310nm and 1550nm Wavelength	47
4.3.1.5	20ml Level Salt Concentration Tested on 1310nm and 1550nm Wavelength	48
4.3.2	Result for Double Loop	49
4.3.2.1	0ml Level Salt Concentration Tested on 1310nm and 1550nm Wavelength	49
4.3.2.2	5ml Level Salt Concentration Tested on 1310nm and 1550nm Wavelength	50
4.3.2.3	10ml Level Salt Concentration Tested on 1310nm and 1550nm Wavelength	51
4.3.2.4	15ml Level Salt Concentration Tested on 1310nm and 1550nm Wavelength	52

4.3.2.5	20ml Level Salt Concentration Tested on 1310nm and 1550nm Wavelength	53
4.4	Comparison between 1310nm and 1550nm for Single Loop	54
4.5	Comparison between 1330nm and 1550nm for Double Loop	55
4.6	Analysis and Result for Microfibre Interaction with Different Level of Salt Concentration Over Time	56
4.6.1	Result for Single Loop	56
4.6.1.1	1 Minutes Tested on 1310nm and 1550nm Wavelength.	57
4.6.1.2	2 Minutes Tested on 1310nm and 1550nm Wavelength.	58
4.6.1.3	3 Minutes Tested on 1310nm and 1550nm Wavelength.	59
4.6.1.4	4 Minutes Tested on 1310nm and 1550nm Wavelength.	60
4.6.1.5	5 Minutes Tested on 1310nm and 1550nm Wavelength.	61
4.6.1.6	6 Minutes Tested on 1310nm and 1550nm Wavelength.	62
4.6.1.7	7 Minutes Tested on 1310nm and 1550nm Wavelength.	63
4.6.2	Result for Double Loop	64
4.6.2.1	1 Minutes Tested on 1310nm and 1550nm Wavelength.	64
4.6.2.2	2 Minutes Tested on 1310nm and 1550nm Wavelength.	65
4.6.2.3	3 Minutes Tested on 1310nm and 1550nm Wavelength.	66
4.6.2.4	4 Minutes Tested on 1310nm and 1550nm Wavelength.	67
4.6.2.5	5 Minutes Tested on 1310nm and 1550nm Wavelength.	68
4.6.2.6	6 Minutes Tested on 1310nm and 1550nm Wavelength.	69
4.6.2.7	7 Minutes Tested on 1310nm and 1550nm Wavelength.	70
4.6.3	Comparison between 1310nm and 1550nm for Single Loop	71
4.6.4	Comparison between 1310nm and 1550nm for Double Loop	72
4.6.5	Average 1310nm and 1550nm for Single Loop	73
4.6.6	Average 1310nm and 1550nm for Double Loop	74
<b>CHAPTER 5</b>	<b>CONCLUSION AND RECOMMENDATIONS</b>	<b>75</b>
5.1	Conclusion	75
5.2	Future Works	76
	<b>REFERENCES</b>	<b>77</b>
	<b>APPENDICES</b>	<b>79</b>

## LIST OF TABLES

<b>TABLE</b>	<b>TITLE</b>	<b>PAGE</b>
Table 2.1	Comparison for previous research paper	20
Table 4.1	Recorded data for 0ml	44
Table 4.2	Recorded data for 5ml	45
Table 4.3	Recorded data for 10ml	46
Table 4.4	Recorded data for 15ml	47
Table 4.5	Recorded data for 20ml	48
Table 4.6	Recorded data for 0ml	49
Table 4.7	Recorded data for 5ml	50
Table 4.8	Recorded data for 10ml	51
Table 4.9	Recorded data for 15ml	52
Table 4.10	Recorded data for 20ml	53
Table 4.11	Recorded data for comparison for different level of concentration (ml) and different wavelength (nm).	54
Table 4.12	Recorded data for comparison for different level of concentration (ml) and different wavelength (nm).	55
Table 4.13	Recorded data for 1 minutes	57
Table 4.14	Recorded data for 2 minutes	58
Table 4.15	Recorded data for 3 minutes	59
Table 4.16	Recorded data for 4 minutes	60
Table 4.17	Recorded data for 5 minutes	61
Table 4.18	Recorded data for 6 minutes	62
Table 4.19	Recorded data for 7 minutes	63
Table 4.20	Recorded data for 1 minutes	64
Table 4.21	Recorded data for 2 minutes	65

Table 4.22 Recorded data for 3 minutes	66
Table 4.23 Recorded data for 4 minutes	67
Table 4.24 Recorded data for 5 minutes	68
Table 4.25 Recorded data for 6 minutes	69
Table 4.26 Recorded data for 7 minutes	70
Table 4.27 Recorded data for output power (dBm) at 1310nm and 1550nm optical light source with different time (m).	71
Table 4.28 Recorded data for output power (dBm) at 1310nm and 1550nm optical light source with different time (m).	72
Table 4.29 Recorded data for average output power (dBm)	73
Table 4.30 Recorded data for average output power (dBm)	74



## LIST OF FIGURES

<b>FIGURE</b>	<b>TITLE</b>	<b>PAGE</b>
Figure 2.1	A typical structure of optical fibre [5]	5
Figure 2.2	Structure of a single-mode fibre[4]	5
Figure 2.3	Structure of multi-mode fibre [4]	6
Figure 2.4	Total internal reflection taking place at the core-cladding interface [5]	7
Figure 2.5	Numerical aperture of optical fibre [9]	8
Figure 2.6	The way light enters and propagates through an optical fibre core [9]	9
Figure 2.7	The effect of strain (compression and tension) on FBG [13]	10
Figure 2.8	Sagnac Circuit [7]	11
Figure 2.9	Setup of two U-bent PO [14]	12
Figure 2.10	Summary of physical measurement that can apply tapered sensors monitoring	16
Figure 3.1	A pair of SC/UPC connectors for Single Mode Fibre Pigtaills	23
Figure 3.2	The jacket and cladding for the optical fibre cable are stripped away with a fibre cutter	24
Figure 3.3	Cleaning tools used for optical fibre cable after stripping process	24
Figure 3.4	Hand cleaver used to cut the fibre tips to the proper length for splicing	25
Figure 3.5	The fusion splicer machine is to splice two fibre together automatically	25
Figure 3.6	The light source that trasmits 1310nm and 1550nm light	26
Figure 3.7	Pulsed laser light flowing via optical fibre is trasmitted and analyze during OTDR testing	26
Figure 3.8	To measure the level of salt concentration	27
Figure 3.9	Salt use for this experiment	27
Figure 3.10	The flowchart of splicing of fibre optic cable	28
Figure 3.11	The flowchart of conducting the experiment in developing fibre optic as a sensor	29

Figure 3.12 Design of a microfiber optic sensor experiment setup at the development phase	30
Figure 3.13 Fibre optic cable being stripped	30
Figure 3.14 Cleaning the bare fibre process	31
Figure 3.15 Cleaving process	31
Figure 3.16 Splicing process	32
Figure 3.17 Tapered process	33
Figure 3.18 Single Loop	33
Figure 3.19 Double Loop	34
Figure 3.20 Testing fibre using laser	34
Figure 3.21 Example of wet to dry cleaning	35
Figure 3.22 Ways to set 0dB reference at power meter	36
Figure 3.23 Insertion loss test	36
Figure 3.24 Example of OTDR testing	37
Figure 3.25 Example of information in the OTDR trace	37
Figure 3.26 The impact of PMD on pulse broadening and potential pulse impairment	39
Figure 3.27 Basic test method for PMD	40
Figure 4.1 New size of the microfiber optic sensor (right)	42
Figure 4.2 Microfiber optic single loop sensor response at 0ml	44
Figure 4.3 Microfiber optic single loop sensor response at 5ml	45
Figure 4.4 Microfiber optic single loop sensor response at 0ml	46
Figure 4.5 Microfiber optic single loop sensor response at 15ml	47
Figure 4.6 Microfiber optic single loop sensor response at 20ml	48
Figure 4.7 Microfiber optic double loop sensor response at 0ml	49
Figure 4.8 Microfiber optic double loop sensor response at 5ml	50
Figure 4.9 Microfiber optic double loop sensor response at 10ml	51

Figure 4.10 Microfiber optic double loop sensor response at 15ml	52
Figure 4.11 Microfiber optic double loop sensor response at 20ml	53
Figure 4.12 Microfiber optic single loop sensor response at 1 minutes	57
Figure 4.13 Microfiber optic single loop sensor response at 2 minutes	58
Figure 4.14 Microfiber optic single loop sensor response at 3 minutes	59
Figure 4.15 Microfiber optic single loop sensor response at 4 minutes	60
Figure 4.16 Microfiber optic single loop sensor response at 5 minutes	61
Figure 4.17 Microfiber optic single loop sensor response at 6 minutes	62
Figure 4.18 Microfiber optic single loop sensor response at 7 minutes	63
Figure 4.19 Microfiber optic double loop sensor response at 1 minutes	64
Figure 4.20 Microfiber optic double loop sensor response at 2 minutes	65
Figure 4.21 Microfiber optic double loop sensor response at 3 minutes	66
Figure 4.22 Microfiber optic double loop sensor response at 4 minutes	67
Figure 4.23 Microfiber optic double loop sensor response at 5 minutes	68
Figure 4.24 Microfiber optic double loop sensor response at 6 minutes	69
Figure 4.25 Microfiber optic double loop sensor response at 7 minutes	70
Figure 4.26 Fiber optic sensor response at both of wavelength	73
Figure 4.27 Fiber optic sensor response at both of wavelength	74

## LIST OF SYMBOLS

$\lambda_B$	-	Bragg wavelength
$\Lambda$	-	Grating Period
$n_{eff}$	-	Effective Refractive Index
$dB$	-	Bandwidth
$\theta_c$	-	Critical Angle
$n_1$	-	Refractive index of the medium around the fiber
$n_2$	-	Refractive index of the cladding



## LIST OF ABBREVIATIONS

V	-	Voltage
RI	-	Reflective Index
$\mu$	-	Micro
k	-	Kilo
M	-	Mega
LAN	-	Local Area Network
FGB	-	Fibre Bragg Gratings
MZI	-	Mach-Zehnder Interference
SI	-	Sagnac Interference
FSR	-	Free Spectral Range
PMF	-	Polarisation-Maintaining Fibre
ASE	-	Amplified Spontaneous Emission
OC	-	Optical Coupler
OSA	-	Spectrum Analyzer
EW	-	Ephemeral Wave Fibre
POF	-	Polymethyl Methacrylate Core
LED	-	Light Emitting Diode
EMI	-	Electromagnetic Interference
RFI	-	Radio Frequency Interference
ASE	-	Amplified Spontaneous Emitter
OTDR	-	Optical Time Division Mirror
NA	-	Numerical Aperture

UNIVERSITI TEKNIKAL MALAYSIA MELAKA  
اوتنور سیتی تیکنیکل ملیسیا ملاک

UNIVERSITI TEKNIKAL MALAYSIA MELAKA

## LIST OF APPENDICES

APPENDIX	TITLE	PAGE
Appendix A	Gantt Chart for PSM 1	79



# CHAPTER 1

## INTRODUCTION

### 1.1 Background

An optical microfiber is one of the optical fibers that are flexible and extremely thin. It is made from transparent glass or plastic. Optical microfiber is widely used in fiber optic communications, which allows transmission over longer distances and at higher bandwidths than electrical cables. Optical microfiber is separate into two which are single-mode fiber were used for long transmission and multimode fiber which is used for short-distance.

There are two types of fiber optic sensors, external fiber optic sensors use a method that transmits the signal from the remote sensor to the data analysis hardware, while fiber optic sensor uses optical fiber as the sensing device. Fiber optic sensor is suitable for noisy and high-vibration environments, as well as extreme heat, humidity, and inherently unstable environment[1]. These fiber optic sensors are ideal for small-scale applications and allow precise positioning of the sensor.

A light source emits a spectrum that is reflected by things recognized by humans' eyes and the brain responds to that signal, which is still used by humans to see. The law of reflectance states that the incident rays, the reflected rays, and the normal must all lie in the same plane. The angle of incidence is equal to the angle of reflection [2]. Due to the change in density between the two substances, the light beam travels from one medium to another by the mechanism of refraction. The relationship between the angle of incidence and the angle of refraction is determined by Snell's law of refraction.

The aim of this project is to create a microfibre double-loop resonator to measure salt concentration. Although there are so many various types of how to measure salt concentration, the focus of this project is to create one of the types to use how to measure salt concentration. Therefore, this project also investigates the effects of fibre optic bending, the bending of a cable that can cause light beams to travel from the fibre, resulting in higher attenuation.

## **1.2 Problem Statement**

Today, the accurate measurement of salt concentrations in liquids is important in a variety of fields, including environmental monitoring, desalination processes, and chemical analysis. However, the existing salt concentration measurement methods are often limited in terms of sensitivity, accuracy, and ease of use of health condition especially in high blood pressure. Therefore, as a result, it was necessary to employ the optical fibre sensor specially designed microfibre double-loop resonator to measure salt concentrations accurately and reliably in liquids.

## **1.3 Project Objective**

The main goal of this project is to measure the concentration of salt water by using the microfibre double-loop resonator. Specifically, the objectives are as follows:

- a) To understand the operation of an Optical Microfibre Double Loop.
- b) To develop Microfibre Double Loop Resonator for Liquid Sensor.
- c) To analyze the performance of Liquid Sensors by Using Optical Microfibre Double Loop Resonator with different levels of concentration.

## 1.4 Scope of Project

The scope of this project are as follows:

- a) Develop and testing with different levels of salt concentration.
- b) Using different wavelength light sources in the optical fibre.
- c) Comparing the result of different levels of concentration.



## CHAPTER 2

### LITERATURE REVIEW

#### 2.1 Introduction

This section includes a full literature review of the project and its development. Additional materials for this project, such as journals, articles, and books of previous work related to the project topic, will serve as the primary source. This chapter will cover everything from fundamentals to related research applications. This step is necessary to grasp the concept of optical fibre and how it works before moving on to the next step, which is developing a microfibre optic sensor for liquid application.

#### 2.2 Fibre Optic

Optical fibres are widely used in our everyday lives, especially in the telecommunication fields. It allows the transmission of data over a longer distance at higher rates. The most apparent applications of optical fibres are for network connection, telephone signals, and so on [1]. It is also used in various fields such as medicine, military, or aerospace. Optical fibres are made of three key elements - core, cladding, and buffer. The core is typically made of quartz glass due to its purity and stability. It is surrounded by a layer of glass or plastic called cladding. The cladding has a lower reflective index (RI) than the core to allow phenomena called total internal reflection to happen and propagation of light within the fibre. The presence of cladding also reduces the loss of light from the core into the surrounding air. It is then surrounded by an elastic layer made of a plastic called buffer, which protects the fibre from physical damage [3]. The fibre optics can be classified based on the mode number – single-mode fibre and multi-mode fibre. It can also be

categorized according to the RI profile – step index and gradient index fibre[3]. Optical fibres are preferable than copper fibres because it allows the transmission of 20 million pulses per second whereas the latter only allows up to a few million pulses per second. [4]

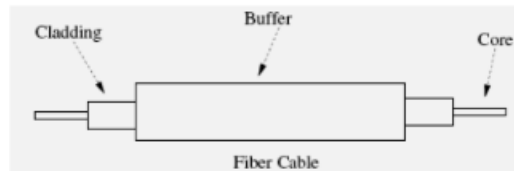


Figure 2.1 A typical structure of optical fibre [5]

### 2.2.1 Single – Mode

Most of the earlier research focused on the development of the multi-mode fibres at 850 nm. However, with the improvement of longer wavelength transmission windows at 1310 and 1550 nm, researchers started focusing on the single-mode fibres [6]. Single-mode or mono-mode fibres have a narrow glass core with a diameter of 8-10  $\mu\text{m}$  and a cladding diameter of 125  $\mu\text{m}$  with a uniform refractive index [7]. It allows only one mode of light to propagate through the core and the movement of light is parallel to the axis, which can reduce the dispersion. These fibres have multiple transmission modes, allowing them to cover distances more than 50 times greater than those achievable by multi-mode fibres. Single-mode fibres are more preferred by the telecommunication company for its high-speed data transmission and higher bandwidth [4]

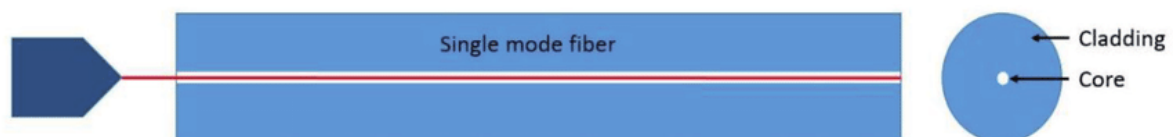


Figure 2.2 Structure of a single-mode fibre[4]

### 2.2.2 Multimode

As the name suggests, multi-mode fibre allows different data transmission to be sent simultaneously within a single fibre. Due to its high numerical aperture and large diameter, the fibre shows efficient coupling from light sources and become the main choice for short distance data transmission. There are two types of multimode fibres – 50  $\mu\text{m}$  core and 62.5  $\mu\text{m}$ . 50  $\mu\text{m}$  core fibre has lower coupling efficiency and was limited to a distance of 1.2 km therefore 62.5  $\mu\text{m}$  core was introduced and it could transmit data up to 100 Mb/s within 2 km [6]. Different modes of light propagate with slightly different travel times, leading to different modes of light arriving at the fibre's output at different times. This distortion is called modal dispersion. As the transmitted light pulses spread at longer fibre lengths, they can overlap with subsequent pulses, creating an interference that will hinder the quality of transmitted signals [1]. Therefore, the multi-modal fibres are now used for shorter distances such as local area networks (LAN) [6].



Figure 2.3 Structure of multi-mode fibre [4]

### 2.3 Propagation of Light Among a Fibre

In fibre optics, the information carrier is a light beam that travels at a speed of  $3 \times 10^8 \text{ m/s}$ , which is far faster and more efficient than electronics in an electric current [5]. The core-to-cladding barrier is where the light pumped into the optical fibre's core propagates. Light will continue to travel along the cable because the cladding is made of a material with a greater refractive index than the core. According to the Snell's Law [8]

### 2.3.1 Total Internal Reflection

The speed at which light travels from one medium to another change, causing the light to change its direction. For example, if the light travels from a higher RI to a medium with a lower RI, it bends away from the normal line and the opposite occurs if the light travels from a lower RI to a medium with a higher RI. Total internal reflection is a phenomenon in which the light will be reflected back upon interaction with a medium with a lower reflective index. The angle at which total internal reflection takes place is called the critical angle. If the angle of incidence (in optical fibres, the angle of incidence is coming from the core) is greater than the critical angle, the light will be reflected back into the glass medium.

When the light enters the core at an angle greater than the critical angle, it will experience total internal reflection at the core-cladding interface. This allows the light to propagate along the length of the fibre.

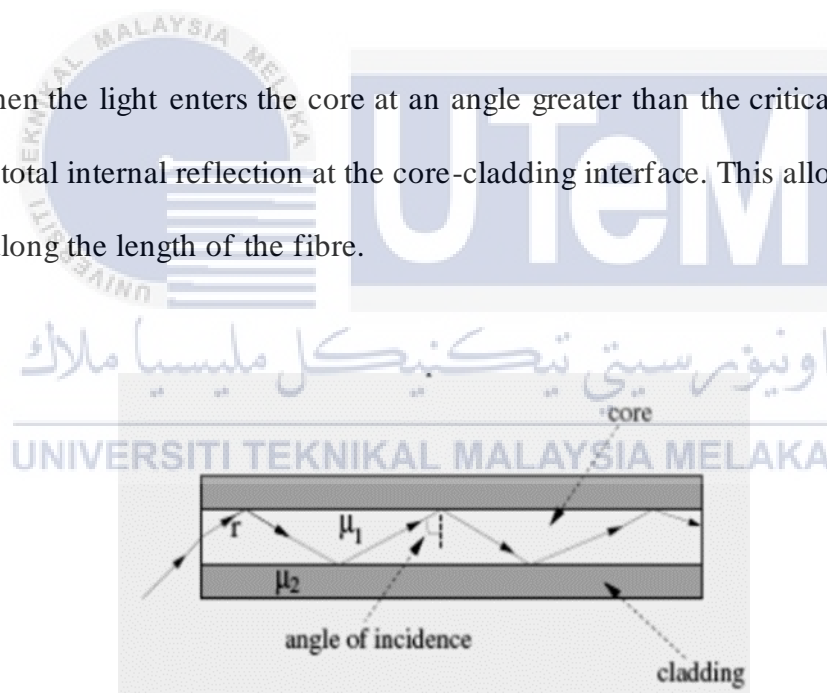


Figure 2.4 Total internal reflection taking place at the core-cladding interface [5]

### 2.3.2 Numerical Aperture

The light ray phenomenon within the optical fibre core has already been explained. Before can get into the core of a fibre optic, it is time to understand the concept of how much light can be received at its entrance. The acceptance angle, also called the maximum angle, is the angle at which something is accepted. Calculate the numerical aperture (NA), the sine of the acceptance angle, and a to determine the acceptance capacity. According to the formula, the difference in refractive indeks between the core and cladding determines the NA.

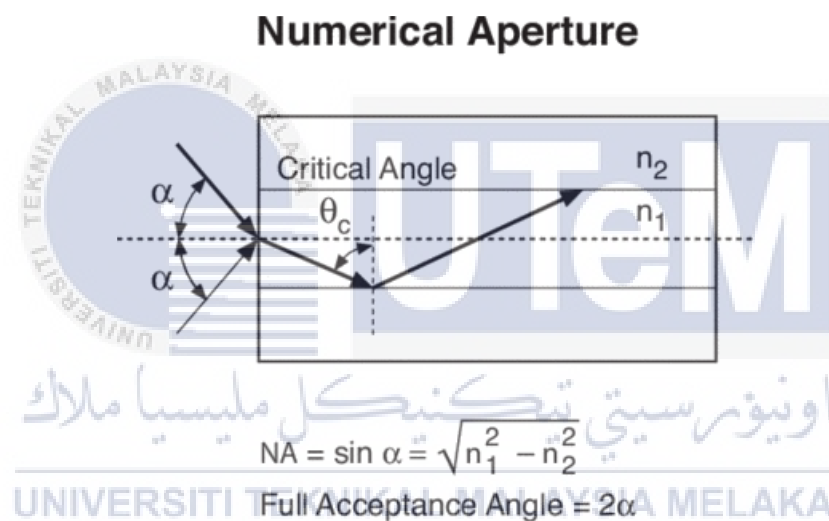


Figure 2.5 Numerical aperture of optical fibre [9]

According to the equation in Figure 2.5, a higher numerical aperture (NA) value corresponds to a larger acceptance angle, indicating that a greater number of light rays are collected. The acceptance cone, or total acceptance angle, will be twice the size of the acceptance angle. This increase in the acceptance angle is beneficial for the efficiency of light coupling, particularly in the implementation of this technology [10].

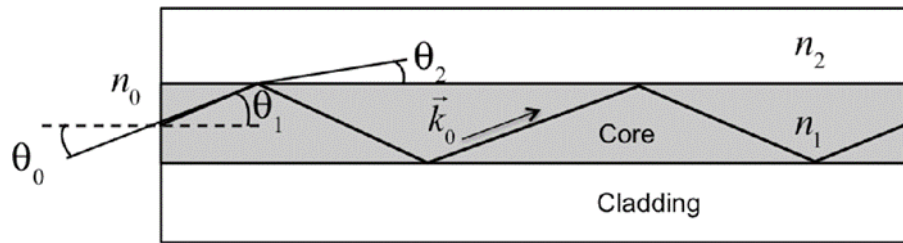


Figure 2.6 The way light enters and propagates through an optical fibre core [9]

According to Figure 2.6, the medium preceding the core is air, which has a refractive index of 1. When light encounters a core with a different refractive index, it undergoes refraction, causing it to bend either away from or toward the normal line, depending on the angle of incidence. Total internal reflection (TIR) takes place within the core.

## 2.4 Various Size of Fibre Optic Sensor

Lately, the industry has seen a rise in the application of optical fibres in sensor technology for sensing different parameters such as temperature, pressure, corrosion, strain, humidity and many more [3]. Optical sensors can identify changes in optical parameters such as RI, reflectance, absorbance, and others which are dependent on the external measurands including pressure, strain, temperature, and many more in the environment. Fibre optic sensors are preferred over conventional sensors because they are unaffected by electromagnetic interference. They can also survive harsh environments and tolerate high temperatures [11]. Fibre optic sensors can be classified into two categories – fibre grating-based sensors such as fibre Bragg gratings (FBG) and interference-based sensors such as Mach-Zehnder interference (MZI) or Sagnac interference (SI) [12]. The following section will focus on fibre Bragg grating and Sagnac interference.

### 2.4.1 High – Resolution Fibre Optic Sensor based on Coated Linearly Chirped Bragg Grating

Fibre Bragg grating (FBG) has garnered significant interest in optical sensing because of its inherent properties including high precision and remarkable sensitivity. During the propagation of light through the core, a section of light rays with a specific wavelength that meets the Bragg condition will be reflected from each grating plane, while the rest are transmitted [13]. The Bragg condition is defined by the following equation:

$$\lambda_B = 2\Lambda n_{eff}$$

Where  $\lambda_B$  is the Bragg wavelength,  $\Lambda$  is the grating period (the distance between two adjacent grating planes) and  $n_{eff}$  is the effective refractive index [13]. The Bragg wavelength is influenced by the grating period and effective refractive index. These variables are affected by external measurands such as strain and temperature. For example, FBG sensors can detect tensile and compressive strains such that the Bragg wavelength will shift to a higher wavelength in response to tensile strain and conversely under the compressive strain (Figure 2.7) [13]

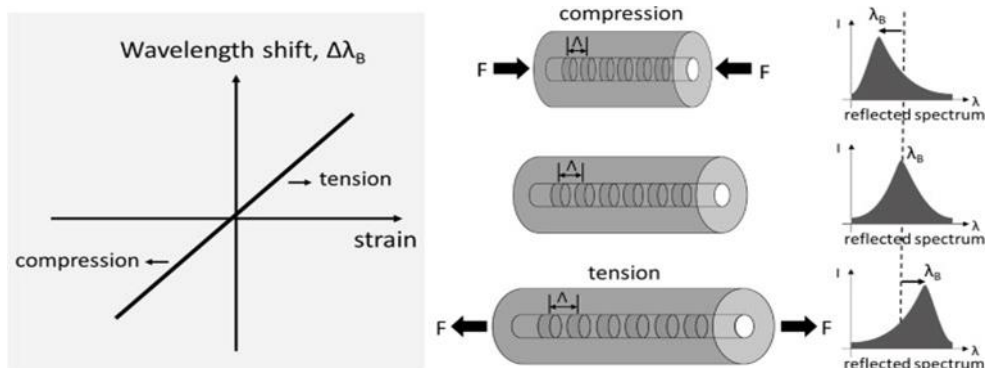
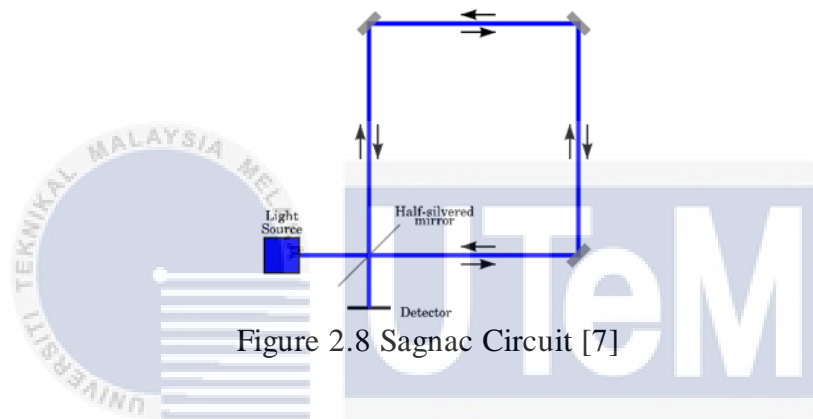


Figure 2.7 The effect of strain (compression and tension) on FBG [13]

## 2.4.2 Sagnac Interference

Sagnac interference or Sagnac effect is based on a phenomenon in which a light is split into several beams and the separated beams are then introduced to the external measurands. They are recombined and the interference pattern is analyzed to determine any phase shift. Sagnac interferometer consists of a light source, a beamsplitter and two detectors placed in opposite directions from the beamsplitter. Sagnac interference sensors is popular due to its property such as high sensitivity, high resolution and convenience



Although Sagnac interferometer-based sensors have high sensitivity, its measurement range is limited because of the free spectral range (FSR) limitation, which is unsuitable for sensing. With this limitation in mind, Liu et al, (2022) designed an optical fibre Sagnac interferometer with polarisation-maintaining fibre (PMF) and a FBG in the loop. By taking advantage of the low sensitivity of the FBG, it is possible to extend the strain detection range, which was initially limited to  $1001 \mu\epsilon$  due to the inability to distinguish the FSR at  $5187 \mu\epsilon$  by combining Sagnac noise with the FBG. Amplified spontaneous emission (ASE) with a bandwidth of 1500-1625 nm emits light in a 2 x 2 3dB (3 dB OC) optocoupler. The input light is divided by 3 dB OC into two beams traveling in opposite directions. The beams are passed through PMF and FBG. After passing the 3dB OC again, the beams interfered with each other to form an interference spectrum recorded with a spectrum analyzer (OSA). Minimum sensitivity to Sagnac strain is  $15.11 \text{ pm}/\mu\epsilon$ , giving a maximum

strain measurement range of  $1058.9\mu\epsilon$ . However, this strain measurement range has not met the needs of actual production and life. The Sagnac is very sensitive but has a narrow measuring range while the FBG series is less sensitive but has a wider measuring range. By cascading PMF with high birefringence and FBG together within the Sagnac ring, strain detection with wide measuring range and high sensitivity can be achieved.

### 2.4.3 Plastic Optical Fibre based Level Sensor Design

Optical fibre liquid level sensor based on optical loss in straight encased optical fibre, the liquid level varies with the increase or decrease of the liquid level due to the change of RI in the area around the optical fibre. To continually monitor the liquid level within a range of 55 cm, use a simple, compact, and susceptible optical fibre level sensor. The POF has a curved U shape with a small diameter (0.5 mm) and a length of  $2L$  ( $L$  is the maximum liquid level). One of the legs serves as a test sensor, detecting variations in light intensity when the liquid level varies. The optoelectronic components are housed in an exceptionally tiny plastic block, which reduces the sensor's footprint and allows it to be carried around with merely electrical input and output connections.

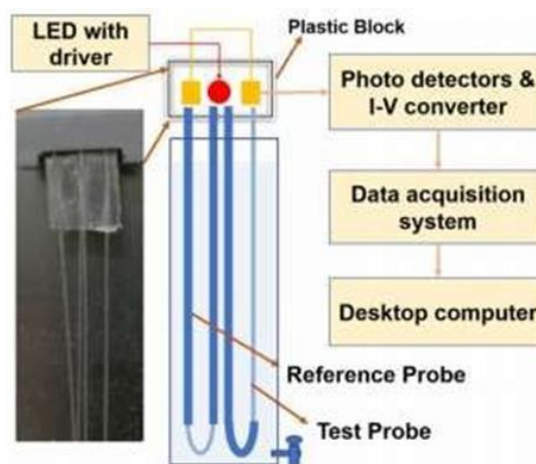


Figure 2.9 Setup of two U-bent PO [14]

#### **2.4.4 Plastic Fibre Optic Sensor of Continuous Liquid Level Monitoring**

Immediate level management is required in many chemical and process companies with storage tanks for long-term storage of water, oil, fuel/oil, and chemicals. Mechanical, Ultrasonic, and electrical engineering are used in most liquid-level sensors on the market. These sensors are mainly used for point measurement and are not suitable for small, interference-prone areas environment, conductive liquids, or hazardous environments. An optical sensor system has been proposed to address these limitations, ensure improved security, reduce maintenance costs, less mechanical parts movement, and continuous liquid level measurement. Ephemeral Wave Fibre (EW) Optical sensing is a low-cost intensity modulation method for monitoring liquid levels in it Optical loss is proportional to liquid level. The low cost, simple handling, optics communication, and reliability of plastic fibre optic sensors have attracted much interest as an alternative to silica fibre. Water and other extraction solutions are used as test liquids in the POF liquid level sensor, which has a dynamic range of over 50 cm and uses an optics fibre test and reference probe test.

##### **2.4.4.1 Material and Method**

This project uses POF (0.5mm, SK20), which has a polymethyl methacrylate core and RI 1.49 and 1.41 stretched fluoropolymers. The distal end of the probe is bent in a U shape to allow optical connection to a pair of LEDs and partial discharge. Our plastic blocks, photovoltaic circuits, and liquid columns form its main part.

#### 2.4.4.2 Discussion

The interaction between the salt ions and the microfibre surface plays an important role. As the salt concentration changes, the refractive index of the solution around the filament changes, causing the resonant wavelength of the device to shift.

One of the advantages of using microfibre to detect liquids, including salt concentrations, is their high sensitivity. The small size of the filament and the long interaction length between the light and the analyte in the ring structure improve detection. This high sensitivity enables detection of low salt concentrations in liquid samples. To implement a microfibre-based salt concentration sensor, several steps need to be taken. First, the microfibre must be fabricated using standard microfabrication techniques. Microfibre is usually made from high-quality optical fibre and its diameter should be in the order of a few micrometers.

After the microfibre is built, it must be functionalized for salt detection. This can be achieved by modifying the surface of the microfibre to improve its interaction with salt ions. Various surface functionalization techniques can be used, such as coating microfibres with specific polymers or capturing specific receptors with an affinity for salt ions.

After the functionalization step, the microfibre is ready to measure the salt concentration. The detection process involves immersing the microfibre in a liquid sample containing salt ions. The microfibre's resonant wavelength is then monitored using an optical setup, such as a spectrometer or an interrogator, and any change in the resonant wavelength is recorded.

To determine the salt concentration, a standard curve is usually constructed. This involves measuring the resonance wavelength shift for different known salt solution concentrations. By comparing the measured deviation with the standard curve, it is possible to define the salt concentration in an unknown sample.

## 2.5 Tapered Optical Fibre

Many other types of sensors have been proposed using fibre optic technology rather than tapered thread, which has attracted much interest due to its wider range of detection and monitoring capabilities and range of features of medical care. Tapered optical fibres have been used for construction couplers to effectively provide light coupling between the fused optical fibres. Today it is used in sensor components, polarizers, light amplifiers, submicron wires, etc. It is recognized as one of the simplest fibre optic sensing components built with excellent sensitivity that was never invented. A short section of an optical fibre can be stretched slightly while heated by the moving burner technique [12], [13] or other methods until the glass becomes flexible to create a tapered thread. Through this process, the thread size can become a few microns narrower in the sub-millimeter to centimeter range. The same amount as the overall sheath of the fibre thins, as does the core of the fibre. This allows ephemeral waves to access mode of propagation and passage through the cone, allowing contact with ambient and measurement properties such as refractive index and ambient variables. According to the characteristics of the descending part, when the diameter of the descending size is reduced, a larger amount of energy from ephemeral waves interacts with the surroundings. It's been since the waveguide of a cone is governed by the profile of the conical sections and the difference in refractive index between the optical fibre and its surroundings. Physics set the measurements that can be monitored using the cone sensor system are summarized in Figure 2.10

Measurand	Taper Geometry	Sensitivity Limit of Detection	Dynamic Range
Temperature	Waist 20 $\mu\text{m}$ LPG ca. 400 $\mu\text{m}$	-0.24 nm/ $^{\circ}\text{C}$	25–75 $^{\circ}\text{C}$
	170 $\mu\text{m}$ 280 $\mu\text{m}$	0.070 nm/ $^{\circ}\text{C}$	0–450 $^{\circ}\text{C}$
	-	46.8 pm/ $^{\circ}\text{C}$	-
	Waist 66.5 $\mu\text{m}$ Length 309 $\mu\text{m}$	9.8 pm/ $^{\circ}\text{C}$	30–100 $^{\circ}\text{C}$
	Waist 97 $\mu\text{m}$ Length 491 $\mu\text{m}$	49.52 pm/ $^{\circ}\text{C}$	20–80 $^{\circ}\text{C}$
	Waist 42 $\mu\text{m}$ Length 2.4 mm	47.37 pm/ $^{\circ}\text{C}$	20–80 $^{\circ}\text{C}$
	Waist 168 $\mu\text{m}$ Length $\mu\text{m}$	57.5 pm/ $^{\circ}\text{C}$	25–70 $^{\circ}\text{C}$
Stress	Waist 165 $\mu\text{m}$ Length 340 $\mu\text{m}$	0.140 nm/ $^{\circ}\text{C}$	30–800 $^{\circ}\text{C}$
	Taper angle 5 $^{\circ}$	0.04 V/GPa	0–0.5 GPa
	Waist 66.5 $\mu\text{m}$ Length 309 $\mu\text{m}$	-6.26 nm/N	0–1 N
Strain	-	1.2 pm/ $\mu\epsilon$	1200 $\mu\epsilon$
	40 $\mu\text{m}$	2000 nm/ $\epsilon$	100–900 $\mu\epsilon$
	-	14 pm/ $\mu\epsilon$	-
	65 $\mu\text{m}$	-183.4 pm/ $\mu\epsilon$	-
	Length 5 mm waist 35 $\mu\text{m}$	22.68 pm/ $\mu\epsilon$	0–400 $\mu\epsilon$
	Waist 168 $\mu\text{m}$ Length 245 $\mu\text{m}$	1.02 pm/ $\mu\epsilon$	81.3–1626 $\mu\epsilon$
	Waist 161 $\mu\text{m}$	0.026 dB/ $\mu\epsilon$	0–590 $\mu\epsilon$
Force	4 $\mu\text{m}$	1900 nm N $^{-1}$	0–0.15 N
Pressure	115–120 $\mu\text{m}$	5.1 pm/bar	0–450 bar
Angle	50 $\mu\text{m}$ Length 44 mm	1 $^{\circ}$	0 $^{\circ}$ –90 $^{\circ}$
	Length 5 mm waist 35 $\mu\text{m}$	185.10 pm/deg	0 $^{\circ}$ –10 $^{\circ}$
	Length 1.37 mm waist 50 $\mu\text{m}$	-4.49 nm/ $^{\circ}$	3 $^{\circ}$ –6.66 $^{\circ}$

Figure 2.10 Summary of physical measurement that can apply tapered sensors monitoring

## 2.6 Sample of Table in Landscape orientation

The two most common types of fibre optic cables used in communication networks are single mode fibre and multimode fibre. Specifications and functions of the specified cable difference type. Although fibre optic cable has been superior to coaxial cable, the technology is still far from perfect. Fibre optic cables offer many advantages over traditional copper cables in a variety of applications. However, its use also comes with certain risks and considerations. Here are the advantages and disadvantages of fibre optic cables:

## Advantages:

- Long-distance signal transmission:

The low attenuation and superior signal integrity found in optical systems allow much longer intervals of signal transmission than metallic-based systems. While single-line, voice-grade copper systems longer than a couple of kilometers (1.2 miles) require in-line signal for satisfactory performance, it is not unusual for optical systems to go over 100 kilometers (km), or about 62 miles, with no active or passive processing.

- Large bandwidth, light weight, and small diameter:

Today's applications require an ever-increasing amount of bandwidth. Consequently, it is important to consider the space constraints of many end users. It is commonplace to install new cabling within existing duct systems or conduit. The relatively small diameter and light weight of optical cable make such installations easy and practical, saving valuable conduit space in these environments.

- Nonconductivity:

Another advantage of optical fibres is their dielectric nature. Since optical fibre has no metallic components, it can be installed in areas with electromagnetic interference (EMI), including radio frequency interference (RFI). Areas with high EMI include utility lines, power-carrying lines, and railroad tracks. All-dielectric cables are also ideal for areas of high lightning-strike incidence.

- Security:

Unlike metallic-based systems, the dielectric nature of optical fibre makes it impossible to remotely detect the signal being transmitted within the cable. The only way to do so is by accessing the optical fibre. Accessing the fibre requires intervention that is easily detectable by security surveillance. These circumstances make fibre extremely attractive to governmental bodies, banks, and others with major security concerns.

- Designed for future applications needs:

Fibre optics is affordable today, as electronics prices fall and optical cable pricing remains low. In many cases, fibre solutions are less costly than copper. As bandwidth demands increase rapidly with technological advances, fibre will continue to play a vital role in the long-term success of telecommunication.

Disadvantages:

- Fragility:

Fibre optic cables are fragile and can be easily damaged by improper handling. They are susceptible to bending, twisting, or excessive stress, which can cause signal loss or damage.

- Cost:

Fibre optic cable is usually more expensive than copper cable. The initial investment in fibre optic infrastructure can be higher, including costs for cabling, specialized equipment, and skilled technicians for installation and maintenance

- **Compatibility:**

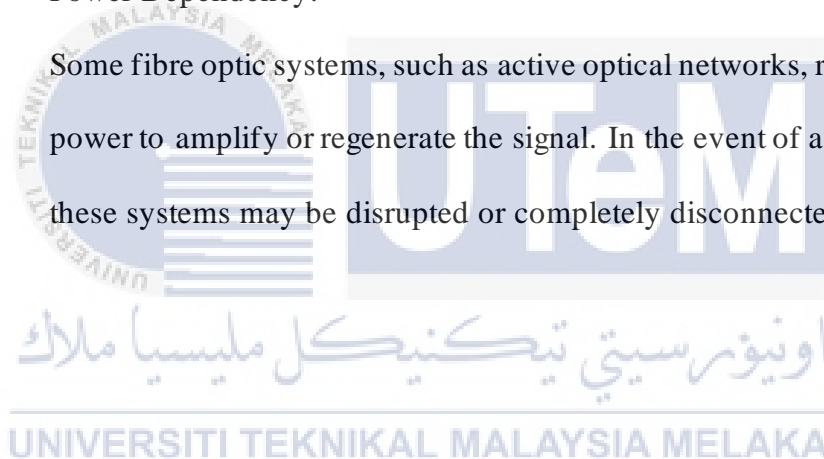
Fibre optic technology may not be compatible with existing infrastructure designed for copper cabling.

- **Limited Flexibility:**

Unlike copper cables, which can be easily terminated and reconnected, fibre optic cables require specialized tools and expertise to terminate. Once installed, it can be more difficult and time consuming to modify or change the fibre optic network.

- **Power Dependency:**

Some fibre optic systems, such as active optical networks, require periodic power to amplify or regenerate the signal. In the event of a power outage, these systems may be disrupted or completely disconnected.



## 2.7 Journal Comparison from Previous Work Related to the Project

Table 2.1 Comparison for previous research paper

No.	Title	Author	Source	Finding
1.	Review of optical fibers-introduction and applications in fiber lasers	[1]	- Fiber optic sensor	Optical fibers, thin, flexible strands, enable efficient light transmission and laser operation in various applications.
2.	Fiber Optic Shape Sensors:A comprehensive review	[2], [3]	- Single mode fiber optic	Study of single mode fiber optic aspects to develop dosimeter for electron beams.
3.	Review on Developments in Fiber Optical Sensors and Applications	[3]	- Fiber optic	Fiber optic sensors offer high sensitivity, immunity, small size, lightweight, remote monitoring.
4.	Introductory Chapter: Optical Fibers	[4]	- Fiber optic	Introduction to optical fibers, covering structure, advantages, components, manufacturing, applications, quality control, and measurements.
5.	SINGLE MODE FIBER STANDARDS: A REVIEW	[5]	- Fiber optic sensors	Using the RI Fabry- Perot fiber optic sensor, compared with the traditional wavelength tracking method, the high resolution of the proposed method was tested when determining the RI
6.	Optical transmission fiber design evolution	[6]	- Single-Mode	Optical transmission fiber design advances for higher data rates, longer distances, and improved performance in modern communication networks.
7.	Fiber Optic Sensors for Harsh and High Radiation Environments in Aerospace Applications	[7]	- Single-Mode	Fiber optic sensors excel in aerospace due to radiation resistance, temperature sensing, distributed sensing, EMI

				immunity, and real-time monitoring.
8.	Tapered Optical Fibre Sensors: Current Trends and Future Perspectives	[11]	- Fibre Optic Sensor	Tapered optical fiber sensors offer enhanced sensitivity, versatile configurations, functional coatings, and nanomaterial integration, enhancing biomedical and environmental sensing performance.
9.	Sagnac interferometer-based optical fiber strain sensor with exceeding free spectral measurement range and high sensitivity	[12]	- Sagnac Interference	Sagnac interferometer based fiber strain sensors achieve high sensitivity and exceed FSR.
10.	Tailoring surface structure and diameter of etched fiber Bragg grating for high strain sensing	[13]	- Bragg Grating	Enhance strain sensing in FBGs through surface structure and diameter modification.
11.	Fiber optic pressure sensor based on a single-mode fiber F-P cavity	[15]	Tapered Optical Fibre	Fiber optic pressure sensors improve sensitivity through diaphragm design, material selection, signal interrogation.
12.	A multi-purpose reflective fiber optic sensor	[14]	- Tapered Optical Fibre	Reflective fiber optic sensor detects environmental changes with enhanced sensitivity, accuracy.
13.	Biomedical application of optical fibre sensors	[8]	- Optical Fibre Sensors	Optical fiber sensors offer diverse biomedical applications due to their small size, high sensitivity, and long-distance transmission capabilities.
14.	Influence of single mode fiber bending on fiber optic gyroscope scale factor stability	[9]	-Single mode fiber optic	Obtain how the single mode fiber bending.
15.	Highly Accurate Refractive Index Sensor Based on Fourier-Transformed Phase Acquisition in Fiber Optic Interferometer	[10]	-Fiber optic sensors	Using the RI Fabry- Perot fiber optic sensor, compared with the traditional wavelength tracking method, the high resolution of the proposed

				method was tested when determining the RI.
--	--	--	--	--

## 2.8 Summary

Various analyzes and methods for liquid sensing using optical fibres have been discussed in this chapter. The focus is on developing fibre optic sensors for liquid sensing applications. Fibre optic sensing technology offers several advantages over traditional sensing methods, making it a viable alternative to liquid sensing.

The review highlights the different methods used in the development of fibre optic fluid sensors. These sensors exploit the unique properties of optical fibres to detect and measure fluid properties such as concentration, level, or composition. The advantages of using fibre optic sensors for liquid detection, including long distance signal transmission, large bandwidth and security are highlighted.

This chapter concludes with an in-depth analysis of the different fibre optic sensing technologies used in the study of liquid sensing, including external and internal methods. External sensing involves the use of external devices or transducers to interact with the fluid, while internal sensing embeds liquid sensing elements directly into the fibre structure. The assessment looks at the organoleptic quality achieved in a controlled laboratory environment, highlighting the advancements and limitations of different approaches.

Overall, the literature review provides an overview of the development and application of fibre optic sensors for liquid sensing. It presents the potential of fibre optic technology in the field and encourages research and exploration of different sensing methods. This chapter is a valuable resource for understanding the most advanced technology in fibre optic fluid sensing and the opportunities for future advancements in the field.

## CHAPTER 3

### METHODOLOGY

#### 3.1 Introduction

A project methodology is a set of principles that quickly describe how a project goes from start to finish. Methods of stripping, cleaving, and splicing fibre optic cables have been discussed in this chapter and the rest of the project. Below is a list of tools needed to complete the process.

##### 1. Single Mode Fibre Pigtails



Figure 3.1 A pair of SC/UPC connectors for Single Mode Fibre Pigtails

## 2. Fibre Cutter and Jacket Remover



Figure 3.2 The jacket and cladding for the optical fibre cable are stripped away with a fibre cutter

## 3. Isopropyl Alcohol



Figure 3.3 Cleaning tools used for optical fibre cable after stripping process

#### 4. Hand Cleaver



Figure 3.4 Hand cleaver used to cut the fibre tips to the proper length for splicing

#### 5. Fusion Splicer



Figure 3.5 The fusion splicer machine is to splice two fibre together automatically

## 6. Amplified Spontaneous Emitter (ASE)



Figure 3.6 The light source that transmits 1310nm and 1550nm light

## 7. Mini Pro Optical Time Domain Reflectometer (OTDR)



Figure 3.7 Pulsed laser light flowing via optical fibre is transmitted and analyzed during OTDR testing

## 8. Measurement Cup



Figure 3.8 To measure the level of salt concentration

## 9. Salt



Figure 3.9 Salt use for this experiment

### 3.2 Project Flow

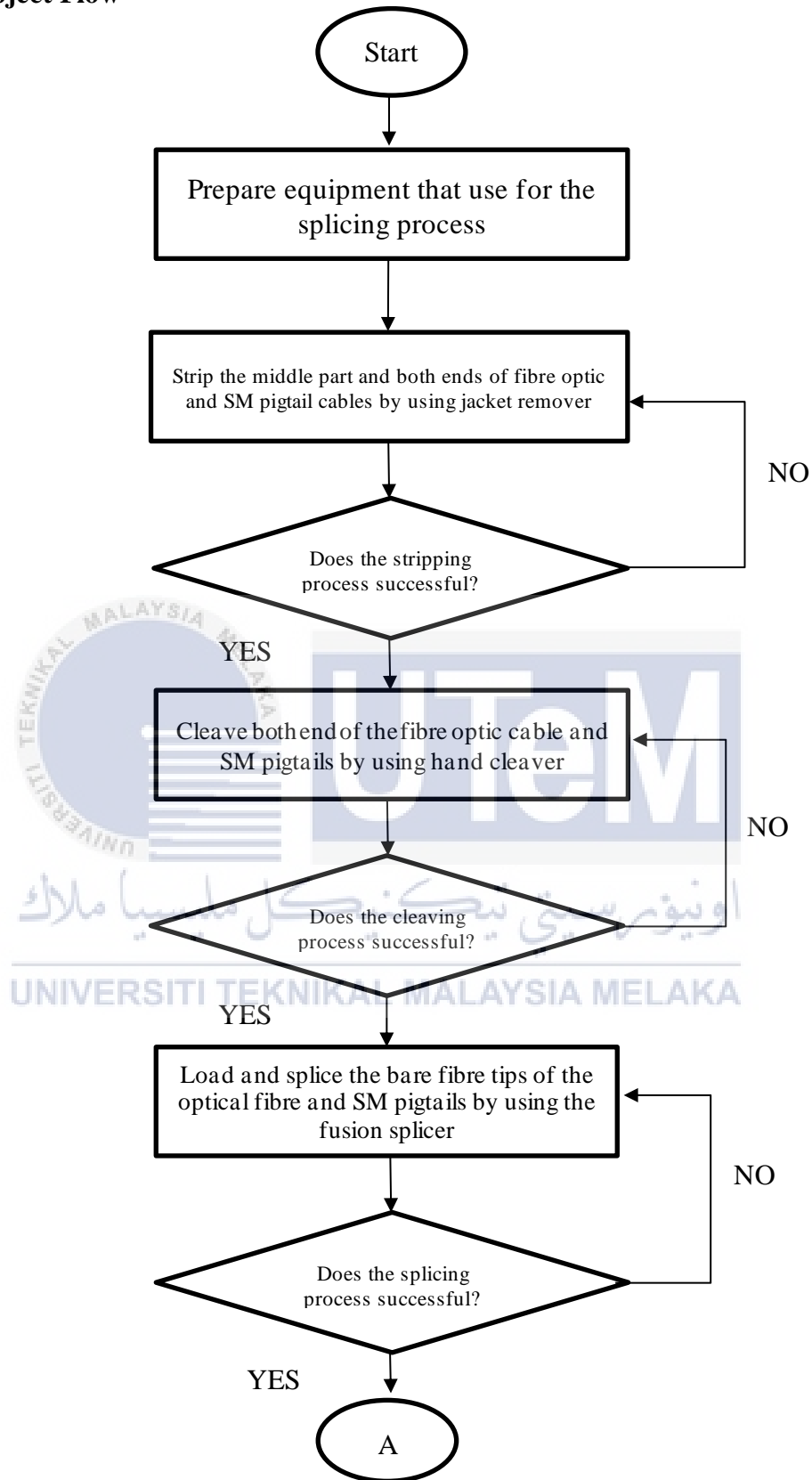


Figure 3.10 The flowchart of splicing of fibre optic cable

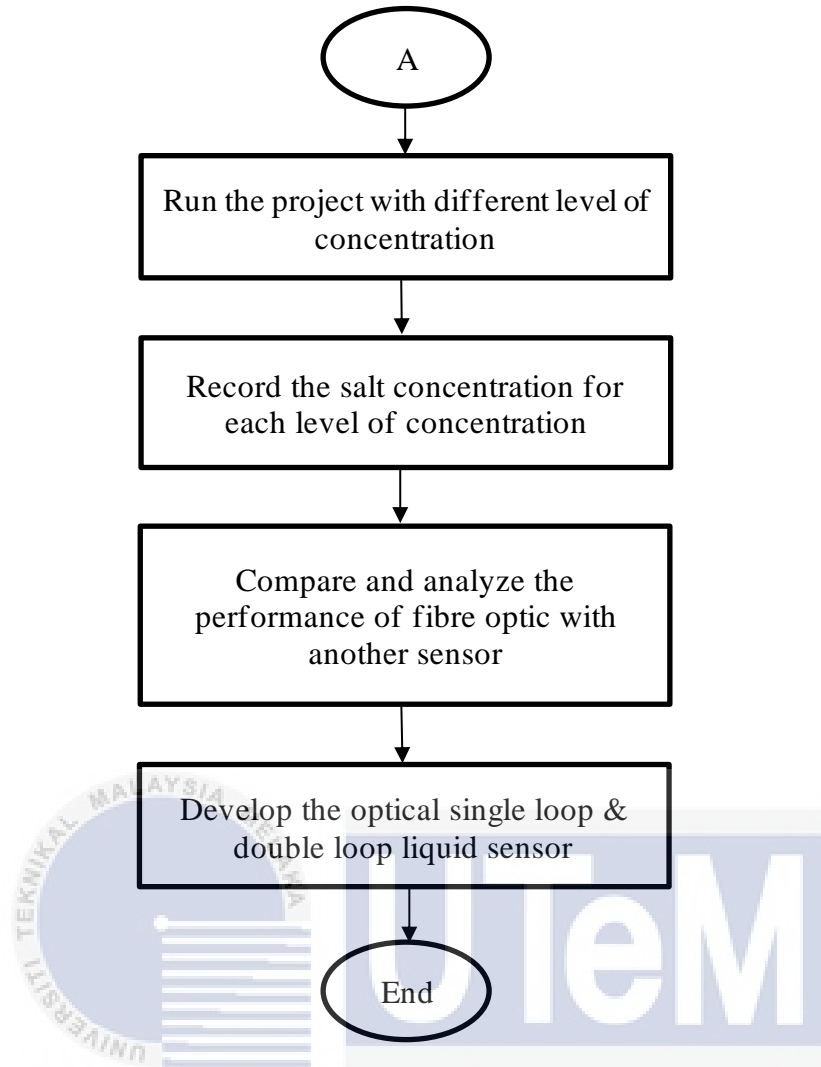


Figure 3.11 The flowchart of conducting the experiment in developing fibre optic as a sensor

### 3.3 Setting up an Experiment with Fibre Optic Sensors

Figure 3.12 shows the test setup of the project. ASE will be transmitter, emitting 1550nm light pulse and OTDR will be receiver, measuring optical power, as shown in the diagram. The optical loop microfibre under test is in the middle.



Figure 3.12 Design of a microfiber optic sensor experiment setup at the development phase

#### 3.3.1 Stripping Process

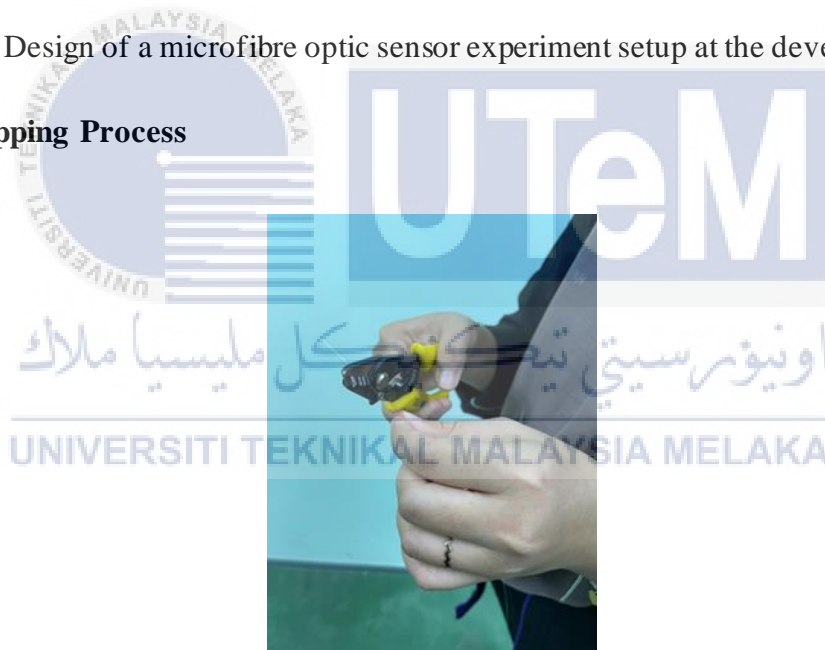


Figure 3.13 Fibre optic cable being stripped

Stripping is the process of removing a protective polymer coating around an optical fibre. Figure 3.2 is a stripping tool used to cut the outer layer before sliding it along to strip the coating. Figure 3.13 shows the stripping process, which removing the coating around an optical fibre in preparation for fusion splicing. The hole in the stripper blade is large enough that the stripper can cut without breaking the fibre glass.

### 3.3.2 Cleaning Process



Figure 3.14 Cleaning the bare fibre process

Once the cladding is removed from the fibre optic cables, the bare fibre should be cleaned by using a piece of free-lint tissue soaked with isopropyl alcohol until it makes a squeaky sound. The purpose is to keep impurities from lingering inside a spliced fibre optic line and causing splice loss. The cleaning procedure follows, as indicated in Figure 3.14.

### 3.3.3 Cleaving Process



Figure 3.15 Cleaving process

During the fibre-cutting process, the surface of the fibre tip may not be a clean, flat surface. Before connecting two fibre optic cables, both ends must be neatly separated by a splitter. This is for a smooth cable connection. The procedure for using the hatchet is described using a splitting process Figure 3.15

### 3.3.4 Splicing process



Figure 3.16 Splicing process

Splicing is the technique of joining two stripped fibre optic cables using a splicing machine. A fibre optic fusion splicer is a machine that uses an electric arc to fuse two of his fibre. Figure 3.16 shows the distance between her two ends of the fibre and the electrode as a guide. Guidance is essential to avoid improper splicing. To achieve the highest transmission speeds, the total loss including splice loss along the cable must be low.

### 3.3.5 Tapered process



Figure 3.17 Tapered process

This process is manufactured and performed to create a microfiber sensor loop. During this process, the core of the fiber is ignited with a special tool created by Dr. Ashadi. This process requires a lot of patience and persistence as there is a risk of affecting the filament if it breaks, breaks and similar to Figure 3.17 shows taper being done.

### 3.3.6 Single Looping Procedure



Figure 3.18 Single Loop

Long-distance transmission in optical fibre communication networks is one of its principal applications. This approach is an extension of self-heterodyne linewidth measurement. It is a setup where the light beam can go around the loop by optical fibres for this looping technique. A long single-mode fibre delay is employed to obtain a reference

signal directly from the laser output, eliminating the need for a separate reference laser. Fibre optic looping is shown in Figure 3.18.

### 3.3.7 Double Looping Procedure



Figure 3.19 Double Loop

This process is used to increase the interaction length and improve the signal structure of the fibre optic cable. By having two microfibre loops, it allows for a higher degree of signal modulation, resulting in a more precise and accurate measurement.

### 3.3.8 Final Check on Fibre

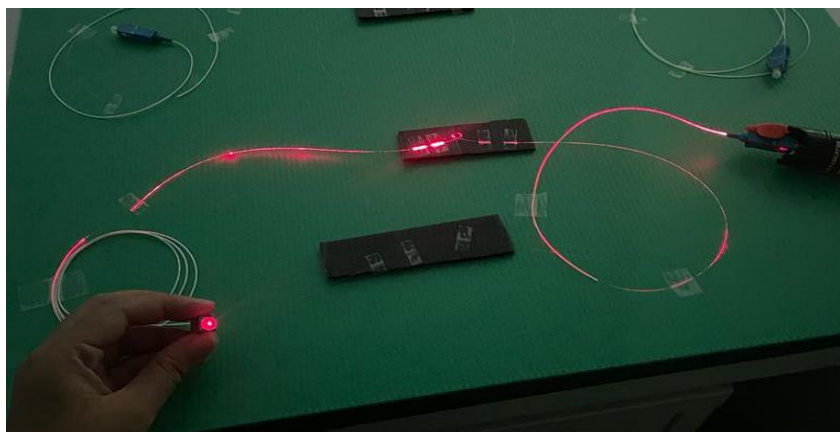


Figure 3.20 Testing fibre using laser

This technique is carried out to ensure the fibre is in good shape. This process is suggested due to concerns over the fibre's condition if it breaks or the laser light does not reach its end. This circumstance is possible because the fibre in question has undergone the taper process, in which the fibre core is burned and transformed into microfiber. Be careful with the fibre's condition if it breaks when looping. The laser test procedure for this fibre sensor is depicted in the diagram (Figure 3.20).

### 3.3.9 Characterization Fibre Optic Loop Sensor

Multiple evaluations of the experimental setup are performed to assess the capabilities when testing this experiment, known as the characterization of fibre optic loop sensor. Fibre characterization examines insertion loss, optical return loss, polarisation, and dispersion to ensure that the fibre can carry traffic and serve as a reference for further debugging and troubleshooting.

### 3.3.10 Connector Inspection



Figure 3.21 Example of wet to dry cleaning

Dirty connectors are issues that might cause receivers to get corrupted due to connector loss. Cleaning the connectors with 99 percent isopropyl alcohol is one option. Cleaning the connectors with cleaning wipes, as shown in Figure 3.21, is another option. The wet part of the wipe will loosen the dirt, while the dry part will wash it away.

### 3.3.11 Insertion Loss Test

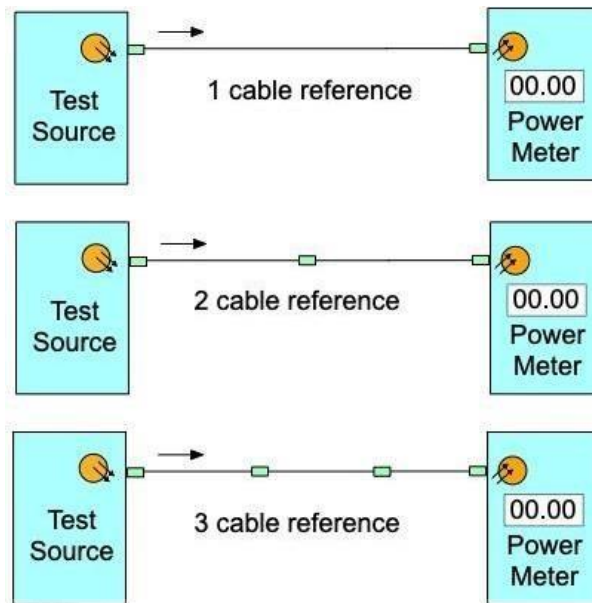


Figure 3.22 Ways to set 0dB reference at power meter

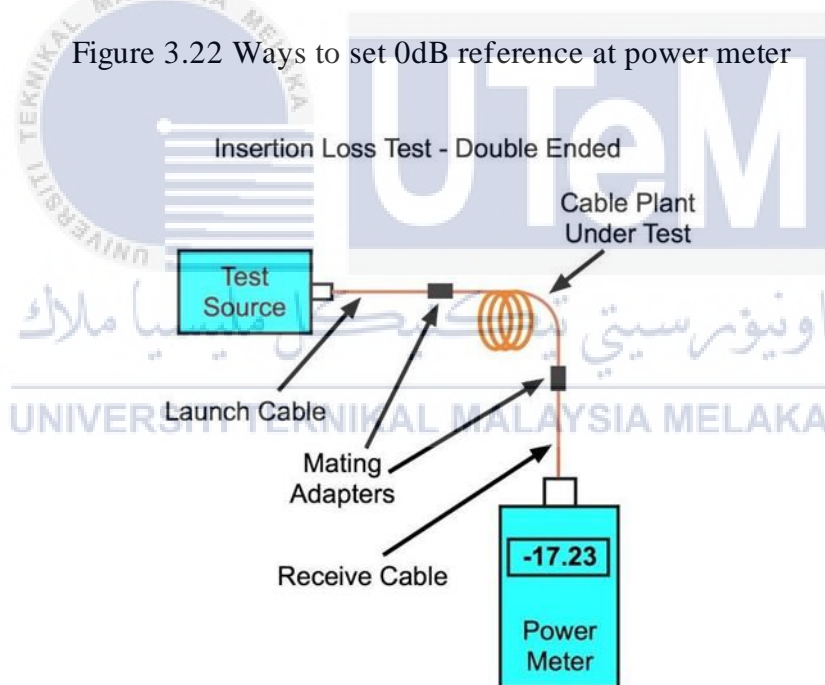


Figure 3.23 Insertion loss test

The insertion loss test aims to recreate the line's working conditions by powering the optical fibre or cable under test with the test source and measuring the attenuation at the other end with the power metre. The test source and power metre are placed between the fibre optic cable and the test source for this experiment. When the source is turned on, the

power meter is set at 0dB as a reference before connecting with the optical fibre used for this project. Figure 3.22 shows an example of setting 0dB reference at the power meter, while Figure 3.23 shows how to test insertion loss.

### 3.3.12 Reflectance or Return Loss Test

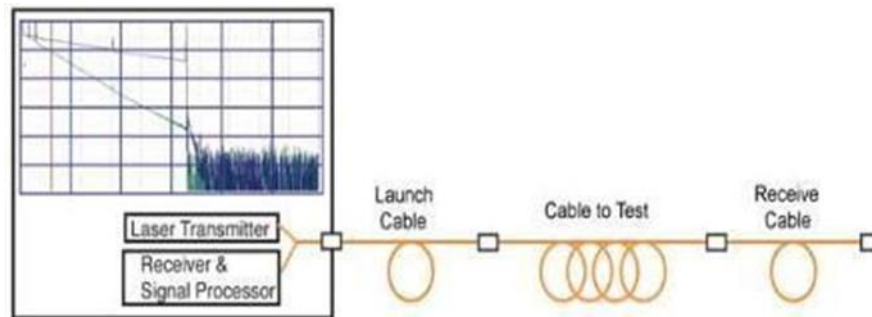


Figure 3.24 Example of OTDR testing

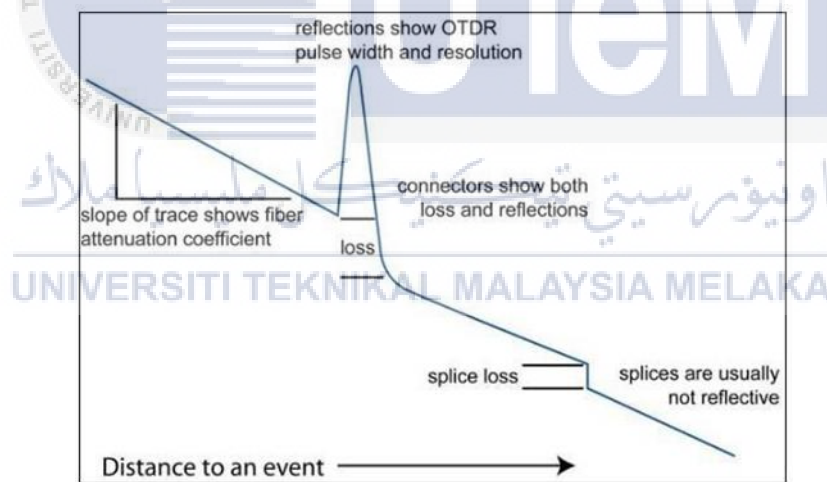


Figure 3.25 Example of information in the OTDR trace

The quantity of light reflected up the fibre toward the source by light reflections off the interface of the polished end surface of the mated connectors and the air is known as reflectance (also known as "back reflection" or optical return loss) of a connection. It is also known as Fresnel reflection, and it is created by light passing through a change in the index of refraction at the fibre ( $n=1.5$ ) and air ( $n=1$ ) interface. Reflectance is primarily a problem

with connectors, but it can also be a problem with mechanical splices that use an index matching gel to eliminate reflection.

Although the term optical return loss is sometimes used interchangeably with the same term reflectance, it has an opposite sign. For instance, the term 50dB return loss is sometimes used to refer to the total amount of backscatter that is collected during a test. However, the manufacturers of optical time-division mirrors (OTDRs) have adopted a different method to measure both return loss and reflectance.

### **3.3.13 Polarization Mode Dispersion**

Polarization mode dispersion (PMD) refers to the fact that the group velocity dispersion of the two orthogonal polarizations in the fibre differs and cannot be adjusted by a single Dispersion compensating fibre (DCF) at the same time. The effect can be attributed to a differential group delay (DGD) between two orthogonally polarised principal states of polarization (PSP) at a particular wavelength or optical frequency for a suitably narrowband source ( Figure 3.26).

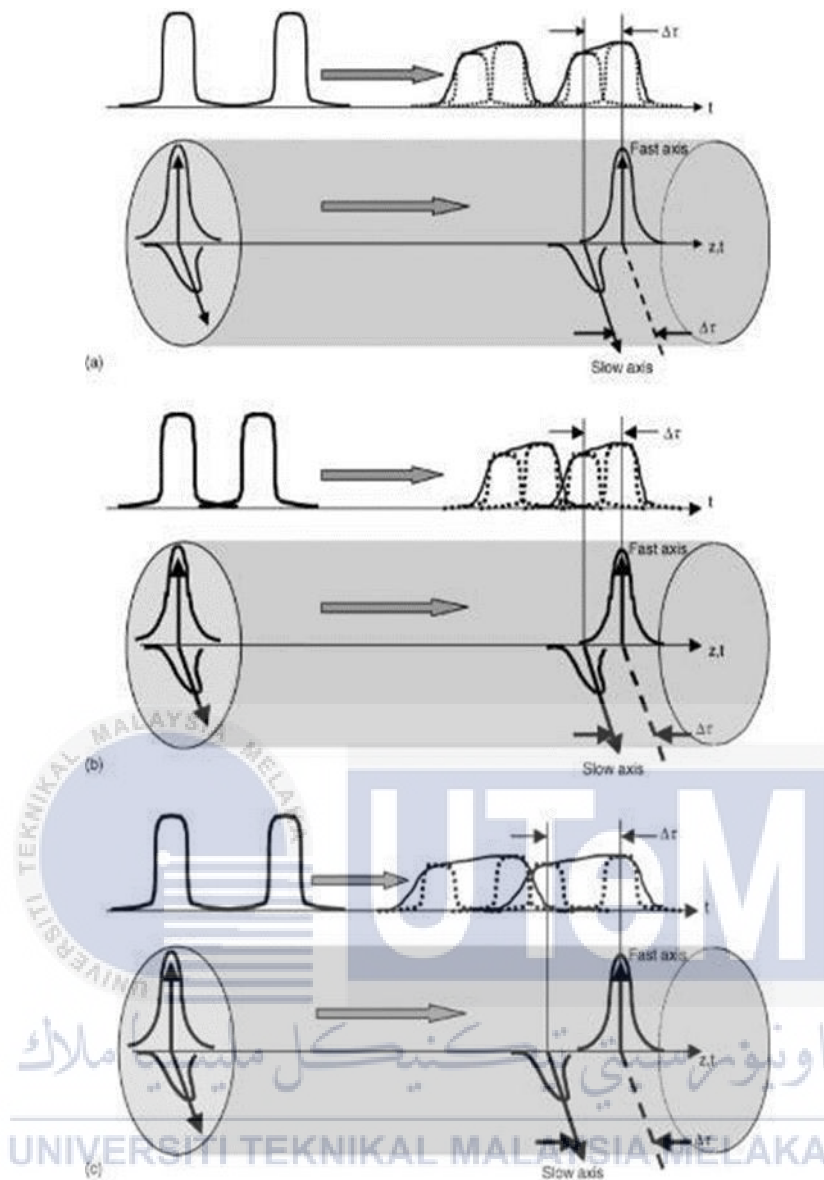


Figure 3.26 The impact of PMD on pulse broadening and potential pulse impairment

- The DGD spreads the pulse, but the bit rate is too low to cause a problem.
- The DGD spreads the pulse, but the bit rate is high enough to cause a problem.
- The DGD is substantial enough to propagate the pulse and cause damage even at modest bit rates.

Fibres are usually tested for PMD during the manufacturing process or while it is being cabled. PMD is commonly tested in the field on newly installed fibres intended for high-speed operation (usually above 2.5 Gb/s) or when upgrading previously installed fibres. Because PMD varies over time, a single test creates an average, and subsequent tests can be performed for comparison. There are various PMD test methods available, some of which are only applicable in the production setting and others which may be utilized in the field. In essence, all test equipment has a source that may modify the polarization of the test signal and a measurement unit that can assess polarisation changes.

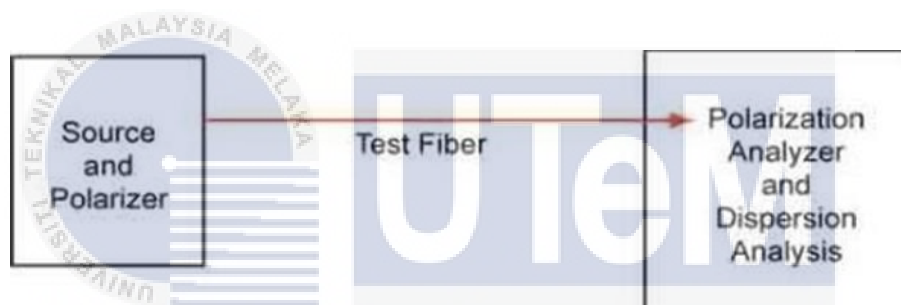


Figure 3.27 Basic test method for PMD

UNIVERSITI TEKNIKAL MALAYSIA MELAKA

### 3.3.14 Summary

In this chapter, the comprehensive flowchart serves as a guide for all activities and tasks. It outlines steps such as preparing optical loop fibers for testing, generating liquid samples with varying different level of concentration, and later, conducting precise optical power readings. The chapter also details the importance of accuracy in readings and provides instructions on cleaning the sensor element using a soft cloth or task wiper soaked in alcohol to eliminate any residual residue or particles. In essence, the method for developing liquid sensors with looped optical fibers, as explained in this chapter, encompasses critical stages delineated in a systematic flowchart. These stages involve preparing the optical loop fiber,

creating liquid samples with diverse liquid levels, ensuring accurate optical power measurements, and preserving sensor performance through meticulous cleaning. Adhering to this methodology facilitates precise experiments, minimizes errors, and ensures dependable outcomes for liquid sensing application.



## CHAPTER 4

### RESULTS AND DISCUSSIONS

#### 4.1 Introduction

The result and data analysis on the creation of the optical microfiber double loop resonator for liquid for medical industry were explained in this chapter. Several tests are used to show how well the project performed. These criteria, which include the sensor's sensitivity and linearity, test results, operational capabilities, and repeatability, will be used to evaluate the sensor's performance. It is crucial to note that the goal of these tests is to support the creation of the sensor.

#### 4.2 Size of Microfiber Optic Loop Sensor

Figure 4.1 shows the new size of the microfiber optic sensor. The size of this microfiber sensor has been measured using a microscope. This microfiber sensor was successfully produced by combustion due to the tapered process. Actual size 125um and successfully reduced to 12.5um.

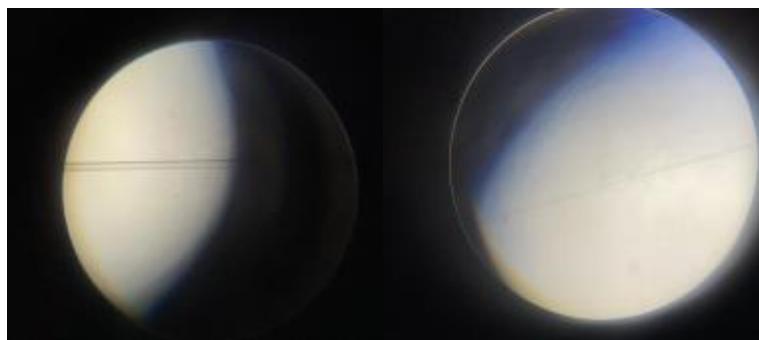


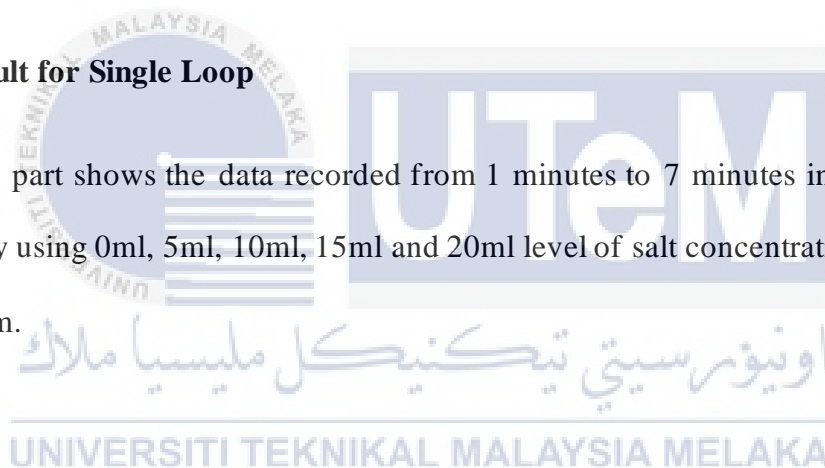
Figure 4.1 New size of the microfiber optic sensor (right)

### 4.3 Result and Analysis for Different Level of Salt Concentration

The experiment entails the transmission of a modulated light source to an optical time domain reflectometer (OTDR) through two single-mode fibre pigtails joined at the splice with a length of an unclad region in the centre of the transmission and a loop. The transmission from the light source would be uneven because some light particles would evaporate from the core of the optical cable. Two types of wavelengths are used in this study, which are 1310nm and 1550nm. This result also contains two different loops with which is single loop and double loop. This study also taken in increments of 1 minute to 7 minutes. The result will vary depending on the level of salt concentration.

#### 4.3.1 Result for Single Loop

This part shows the data recorded from 1 minutes to 7 minutes in a single loop resonator by using 0ml, 5ml, 10ml, 15ml and 20ml level of salt concentration on 1310nm and 1550nm.



### 4.3.1.1 0 ml Level Salt Concentration Tested on 1310nm and 1550nm Wavelength

Table 4.1 Recorded data for 0ml

Output Power 0 ml level salt concentration (dBm)		
Time	1310 nm	1550 nm
1	41.36	35.43
2	43.87	36.57
3	44.54	36.73
4	45.02	36.75
5	45.13	36.77
6	45.19	36.77
7	45.31	36.78

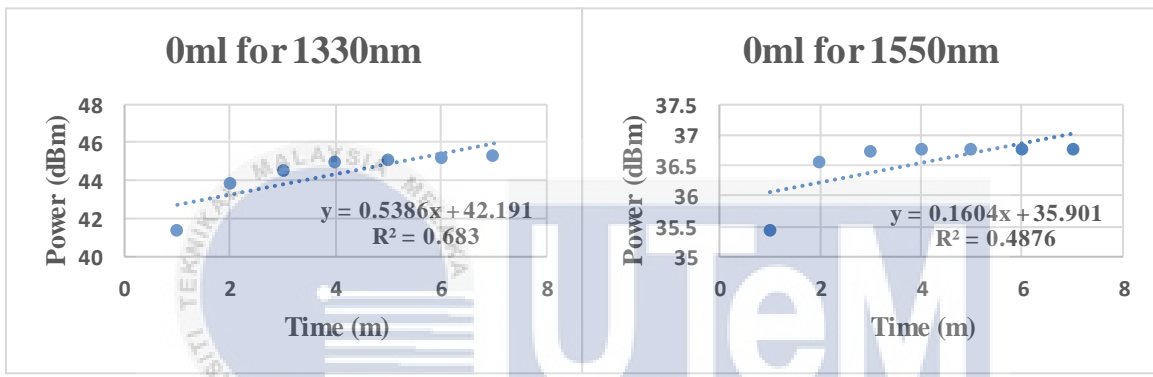


Figure 4.2 Microfiber optic single loop sensor response at 0ml

The table and graph depict an increase in value for both wavelengths. For the optical light source at 1310nm, there is a significant rise, with a gradient of 0.5386, while for the 1550nm optical light source, it is 0.1604. Upon comparison, it can be concluded that, at a 0ml level of salt concentration, 1310nm is more sensitive than 1550nm.

### 4.3.1.2 5ml Level Salt Concentration Tested on 1310nm and 1550nm Wavelength

Table 4.2 Recorded data for 5ml

Output Power 5 ml level salt concentration (dBm)		
Time	1310 nm	1550 nm
1	44.36	36.51
2	46.56	39.11
3	46.88	39.59
4	46.98	40.01
5	47.26	40.13
6	47.35	40.14
7	47.42	40.19

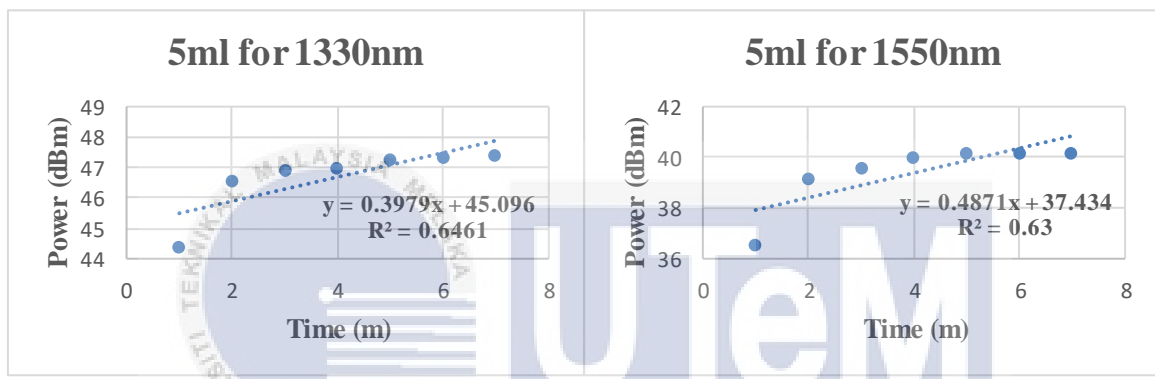


Figure 4.3 Microfiber optic single loop sensor response at 5ml

From Figure 4.2 for comparison, at a 0ml level of salt concentration, 1310nm appears more sensitive than 1550nm. However, at 5ml, a different trend emerges. It can be concluded that 1550nm is more sensitive because the gradient is 0.4871 compared to 1310nm, which registers a lower value of 0.3979. This suggests that the sensitivity of the wavelengths may vary at different salt concentrations, with 1550nm exhibiting higher sensitivity at 5ml.

### 4.3.1.3 10ml Level Salt Concentration Tested on 1310nm and 1550nm Wavelength

Table 4.3 Recorded data for 10ml

Output Power 10ml level salt concentration (dBm)		
Time	1310 nm	1550 nm
1	48.33	39.9
2	48.61	40.7
3	48.99	40.9
4	49.1	40.95
5	49.29	40.96
6	49.62	41.01
7	50.05	41.06

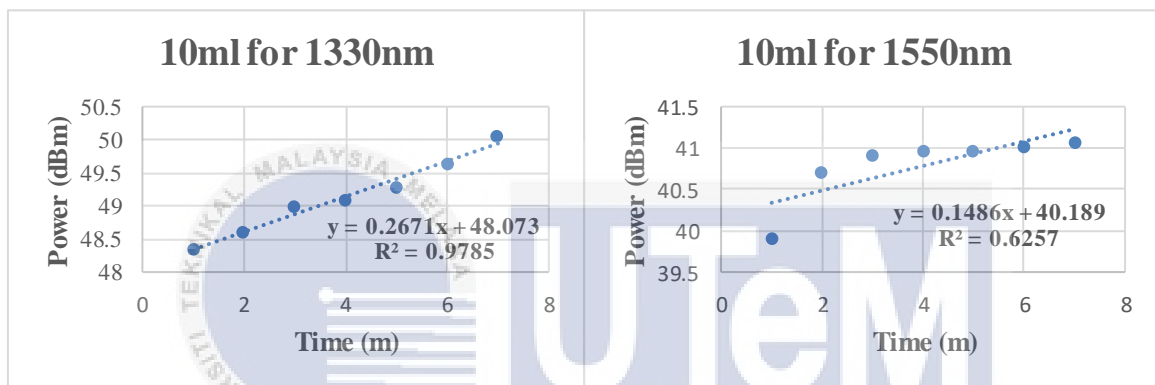


Figure 4.4 Microfiber optic single loop sensor response at 0ml

In the Table 4.3, data has been recorded for the salt concentration level of 10 ml. For the 1310nm optical light source, the output power value increase by only 1.72, going from 48.33 dBm to 50.05 dBm. Meanwhile, for the 1550nm optical light source, the increase is 1.16 dBm, moving from 39.90 dBm to 41.06 dBm. The Figure 4.4 illustrates the sensor response at the 10 ml salt concentration level. In terms of sensitivity testing for both wavelengths at this concentration level, the 1310nm wavelength achieved the highest gradient, reaching 0.2671, compared to the 1550nm wavelength, which reached 0.1486.

#### 4.3.1.4 15ml Level Salt Concentration Tested on 1310nm and 1550nm Wavelength

Table 4.4 Recorded data for 15ml

Output Power 15ml level salt concentration (dBm)		
Time	1310 nm	1550 nm
1	49.1	35.04
2	50	36.29
3	50.24	36.45
4	50.89	36.48
5	51.08	36.5
6	51.24	36.5
7	51.31	36.5

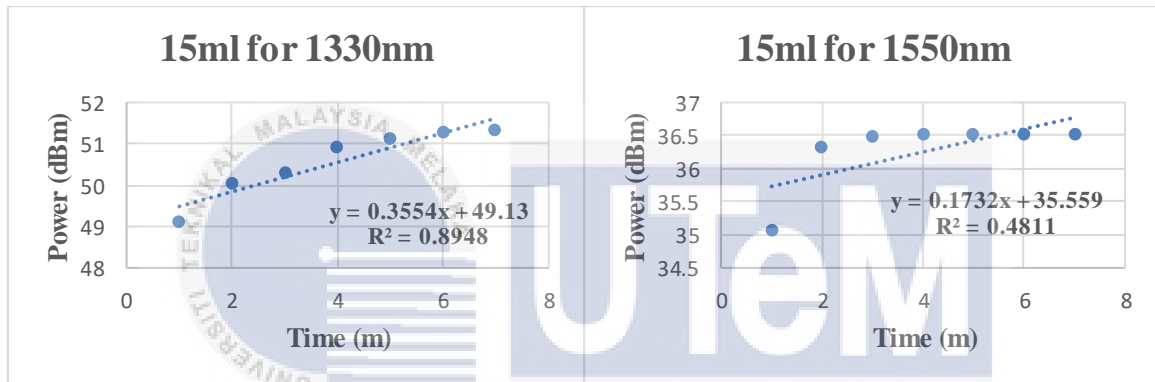


Figure 4.5 Microfiber optic single loop sensor response at 15ml

The table displays output power data (dBm) for a 15ml salt concentration level at various times. Both wavelengths of the optical light source exhibit an increase in output power values (dBm). However, the difference for each wavelength varies from minute 1 to minute 7. For the 1310nm wavelength, the difference from minute 1 to minute 7 is 2.21 dBm, while for the 1550nm wavelength, it is 1.46 dBm. The figure illustrates the sensor's response to a 15ml salt concentration level at different times. At this concentration level, the 1310nm wavelength is more responsive to concentration, showing a gradient value of 0.3554, while the 1550nm wavelength is at 0.1732.

### 4.3.1.5 20ml Level Salt Concentration Tested on 1310nm and 1550nm Wavelength

Table 4.5 Recorded data for 20ml

Output Power 20ml level salt concentration (dBm)		
Time	1310 nm	1550 nm
1	50.47	36.57
2	50.58	36.57
3	51.37	36.82
4	51.69	36.82
5	52.4	36.86
6	55.13	36.88
7	55.76	36.88

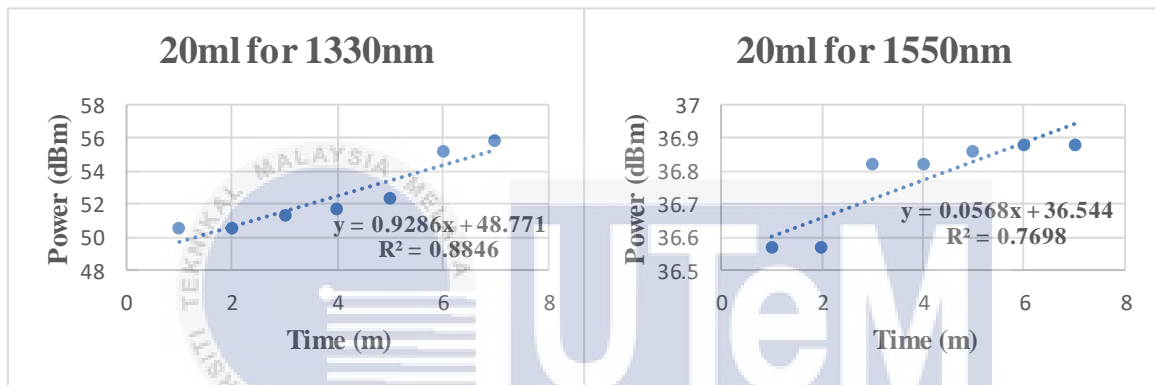


Figure 4.6 Microfiber optic single loop sensor response at 20ml

The Table 4.5 presents data on output power (dBm) at different times for a 20ml salt concentration. The output power (dBm) increase for both wavelengths of the optical light source. From minute 1 to minute 7, the difference for each wavelength varies. The disparity between minute 1 and minute 7 is 0.31 dBm for the 1550 nm wavelength, while it is 5.29 dBm for the 1310 nm wavelength. In Figure 4.6, the sensor's response to a 20ml salt concentration at various times is illustrated. At this salt concentration level, the 1550 nm wavelength has a gradient value of 0.0568, while the 1310 nm wavelength has a gradient value of 0.9286. It can be concluded that, at 20ml level of salt concentration 1310nm is more sensitive than 1550nm.

### 4.3.2 Result for Double Loop

This part shows the data recorded from 1 minutes to 7 minutes in a double loop resonator by using 0ml, 5ml, 10ml, 15ml and 20ml level of salt concentration on 1310nm and 1550nm.

#### 4.3.2.1 0ml Level Salt Concentration Tested on 1310nm and 1550nm Wavelength

Table 4.6 Recorded data for 0ml

Output Power 0 ml level salt concentration (dBm)		
Time	1310 nm	1550 nm
1	41.94	37.68
2	42.77	38.82
3	43.66	40.11
4	43.89	40.41
5	44.26	40.5
6	44.98	40.52
7	45.56	40.53

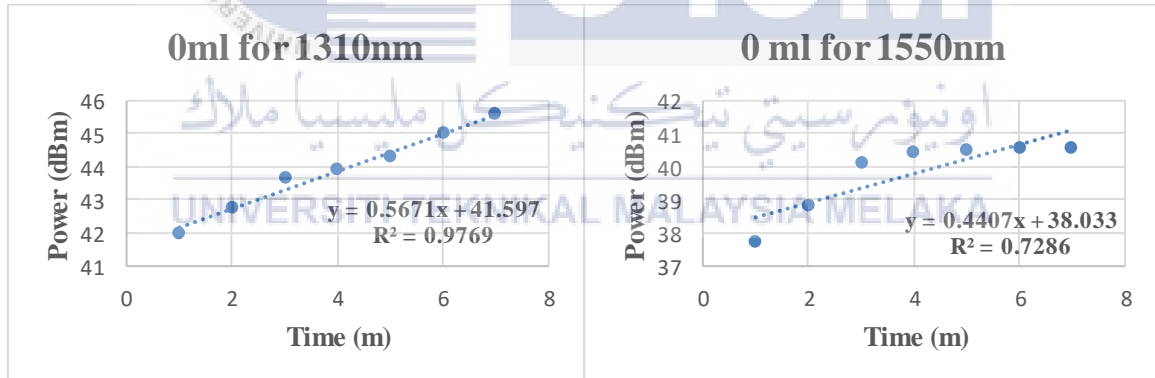


Figure 4.7 Microfiber optic double loop sensor response at 0ml

The Table 4.6 presents data on output power (dBm) at different times for a 0ml salt concentration level. The output power (dBm) increases for both wavelengths of the optical light source. However, from minute 1 to minute 7, the difference varies depending on the wavelength. The disparity between minute 1 and minute 7 is 3.62 dBm for the 1310 nm wavelength, while for the 1550 nm wavelength, it is 2.85 dBm. Figure 4.7 shows the sensor's response to a 0ml salt

concentration level at various times. With a gradient value of 0.5671 at a 0ml salt concentration level, the 1310 nm wavelength is more responsive to concentration than the 1550 nm wavelength, which has a gradient value of 0.4407.

#### 4.3.2.2 5ml Level Salt Concentration Tested on 1310nm and 1550nm Wavelength

Table 4.7 Recorded data for 5ml

Output Power 5 ml level salt concentration (dBm)		
Time	1310 nm	1550 nm
1	44.18	38.77
2	45.01	39.08
3	45.18	40.18
4	45.26	40.24
5	45.36	40.32
6	45.89	40.33
7	46.2	40.38

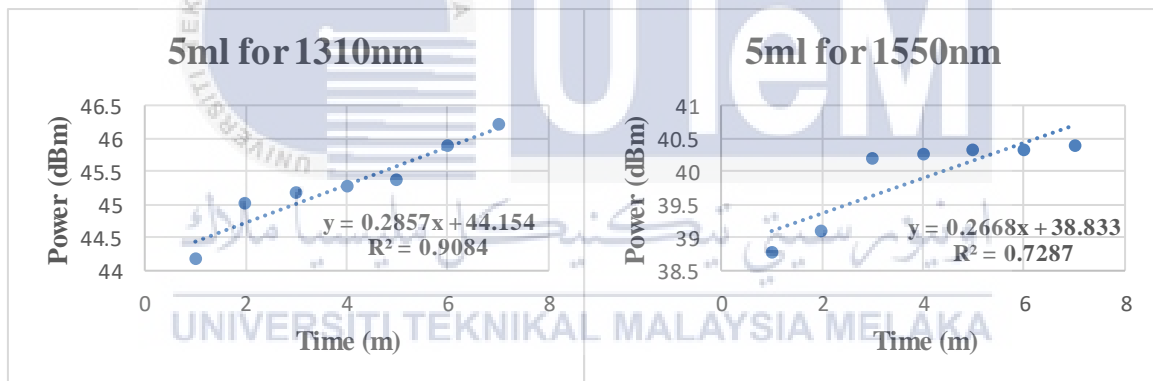


Figure 4.8 Microfiber optic double loop sensor response at 5ml

Data for output power (dBm) with a 5ml level of salt concentration at various times are presented in Table 4.7. The output power (dBm) experiences reduction under the influence of two wavelengths from the optical light source. Between minute 1 and minute 7, the disparity for each wavelength fluctuates. Specifically, the difference between minute 1 and minute 7 for the 1310 nm wavelength is 2.02 dBm, while for the 1550nm wavelength, it is 1.61 dBm. Figure 4.8 illustrates the sensor's response to a 5ml level of salt concentration

at different times. Notably, the 1310 nm wavelength exhibits a gradient value of 0.2857, while the 1550 nm wavelength has a gradient value of 0.2668.

#### 4.3.2.3 10ml Level Salt Concentration Tested on 1310nm and 1550nm Wavelength

Table 4.8 Recorded data for 10ml

Output Power 10 ml level salt concentration (dBm)		
Time	1310 nm	1550 nm
1	43.52	39.7
2	45.04	39.86
3	45.43	39.98
4	45.49	40.01
5	45.53	40.07
6	45.63	40.08
7	45.63	40.1

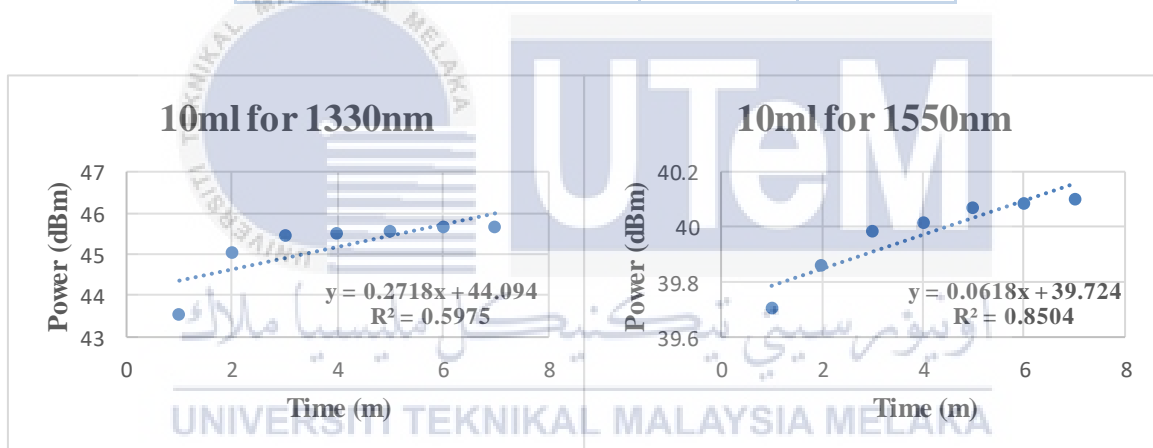


Figure 4.9 Microfiber optic double loop sensor response at 10ml

The table and graph above depict an increase in value for both wavelengths. Specifically, the gradient for the optical light source at 1310 nm is 0.2718, whereas for the 1550 nm optical light source, it is 0.0618. In contrast, it can be inferred that, for a 10ml level of salt concentration, the sensitivity of 1310 nm surpasses that of 1550 nm.

#### 4.3.2.4 15ml Level Salt Concentration Tested on 1310nm and 1550nm Wavelength

Table 4.9 Recorded data for 15ml

Output Power 15 ml level salt concentration (dBm)		
Time	1310 nm	1550 nm
1	40.87	38.46
2	42.54	39.43
3	42.89	40.33
4	43.12	40.49
5	43.17	40.56
6	43.19	40.63
7	43.24	40.69

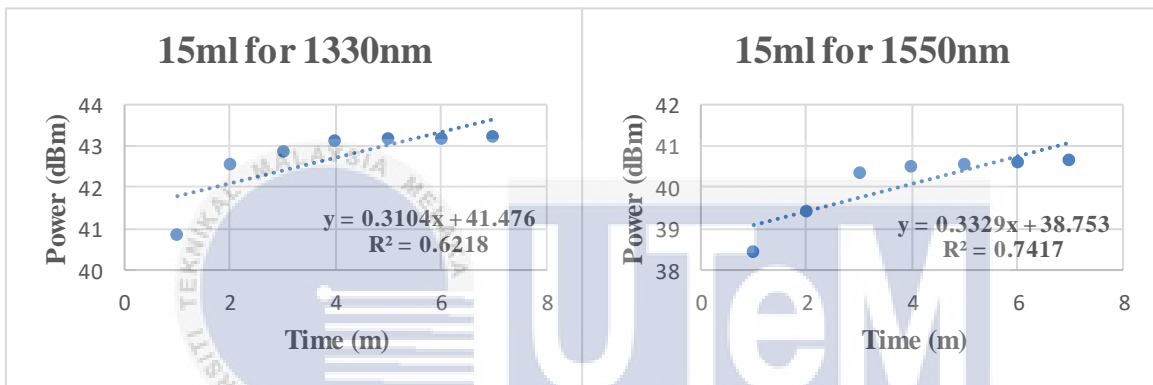


Figure 4.10 Microfiber optic double loop sensor response at 15ml

Table 4.9 displays output power data (dBm) for a 15ml level of salt concentration at various times. The two wavelengths of the optical light source exhibit a reduction in the output power value (dBm). However, the difference for each wavelength varies from minute 1 to minute 7. For the 1310 nm wavelength, the difference from minute 1 to minute 7 is 2.37 dBm, while for the 1550 nm wavelength, it is 2.23 dBm. Figure 4.10 illustrates the sensor's response to a 15ml level of salt concentration at different times. Notably, at the 15ml level of salt concentration, wavelength 1550 nm demonstrates a higher responsiveness to concentration with a gradient value of 0.3329, whereas wavelength 1310 nm exhibits a gradient value of 0.3104.

### 4.3.2.5 20ml Level Salt Concentration Tested on 1310nm and 1550nm Wavelength

Table 4.10 Recorded data for 20ml

Output Power 20 ml level salt concentration (dBm)		
Time	1310 nm	1550 nm
1	41.4	38.89
2	43.26	39.48
3	43.41	39.87
4	43.5	40
5	43.56	40.02
6	43.56	40.07
7	43.57	40.11

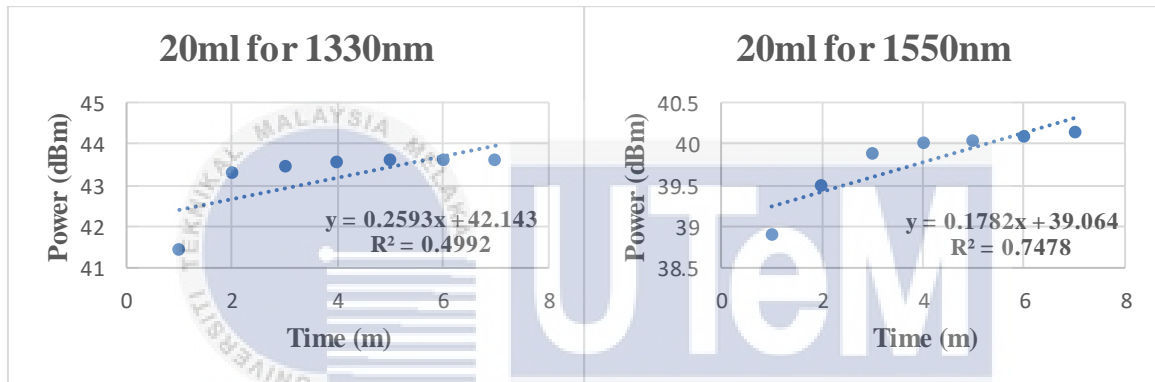


Figure 4.11 Microfiber optic double loop sensor response at 20ml

In Table 4.10, data has been recorded for the humidity percentage at a 20-level salt concentration. For the 1310nm wavelength optical light source, the output power value decreases by only 2.17, transitioning from 41.4 dBm to 43.57 dBm. Conversely, for the 1550nm wavelength optical light source, the decrease is 1.22 dBm, going from 38.39 dBm to 40.11 dBm. Figure 4.11 illustrates the sensor response at the salt concentration level. Regarding sensitivity testing for both wavelengths at the 20-level salt concentration, the 1310nm wavelength reached a higher value in its gradient at 0.2593, compared to the 1550nm wavelength at 0.1782.

#### 4.4 Comparison between 1310nm and 1550nm for Single Loop

Table 4.11 Recorded data for comparison for different level of concentration (ml) and different wavelength (nm).

Level of Salt Concentration (ml)	1310nm		1550nm	
	Sensitivity (dBm)	Linearity (%)	Sensitivity (dBm)	Linearity (%)
0	0.5386	82.64	0.1604	69.83
5	0.3979	80.38	0.4871	79.37
10	0.2671	98.92	0.1486	79.10
15	0.3554	94.60	0.1732	69.36
20	0.9286	94.05	0.0568	87.74

The results for different level of salt concentration have been recorded in 1 table. Table 4.11 shows the output power values for each optical light source which are 1310nm and 1550nm. From this table, it can be concluded that at 1310nm, 20ml level of salt concentration is more sensitive than other level of concentration and reaches the highest value of 0.9286. The use of 1550nm wavelength optical light source, at 5ml level of concentration, is more sensitive than that other, which is 0.4871.

#### 4.5 Comparison between 1330nm and 1550nm for Double Loop

Table 4.12 Recorded data for comparison for different level of concentration (ml) and different wavelength (nm).

Level of Salt Concentration (ml)	1310nm		1550nm	
	Sensitivity (dBm)	Linearity (%)	Sensitivity (dBm)	Linearity (%)
0	0.5671	98.83	0.4407	85.35
5	0.2857	95.31	0.2668	85.36
10	0.2718	77.30	0.0618	92.22
15	0.3104	78.85	0.3329	86.12
20	0.2593	70.65	0.1782	86.46

The results for different levels of salt concentration have been compiled in Table 4.12. This table presents the output power values for each optical light source, namely 1310nm and 1550nm. A conclusion drawn from this table is that at 1310nm, the 0ml level of salt concentration exhibits higher sensitivity compared to other concentration levels, reaching the maximum value of 0.5671. Similarly, the use of the 1550nm wavelength optical light source indicates that, at the 0ml level of concentration, it is more sensitive than others, registering a value of 0.4407.

#### **4.6 Analysis and Result for Microfibre Interaction with Different Level of Salt Concentration Over Time**

This section contains data collected at various times, ranging from one minute to seven minutes, with one-minute intervals at varying level of salt concentration.

##### **4.6.1 Result for Single Loop**

This part shows the data recorded by using 0ml, 5ml, 10ml, 15ml and 20ml level of salt concentration on 1310nm and 1550nm from 1 minutes to 7 minutes in a single loop resonator.



#### 4.6.1.1 1 Minutes Tested on 1310nm and 1550nm Wavelength.

Table 4.13 Recorded data for 1 minutes

Output Power of 1 minutes (dBm)		
Level of salt concentration (ml)	1310nm	1550nm
0	41.36	35.43
5	44.36	36.51
10	48.33	39.9
15	49.1	35.04
20	50.47	36.57

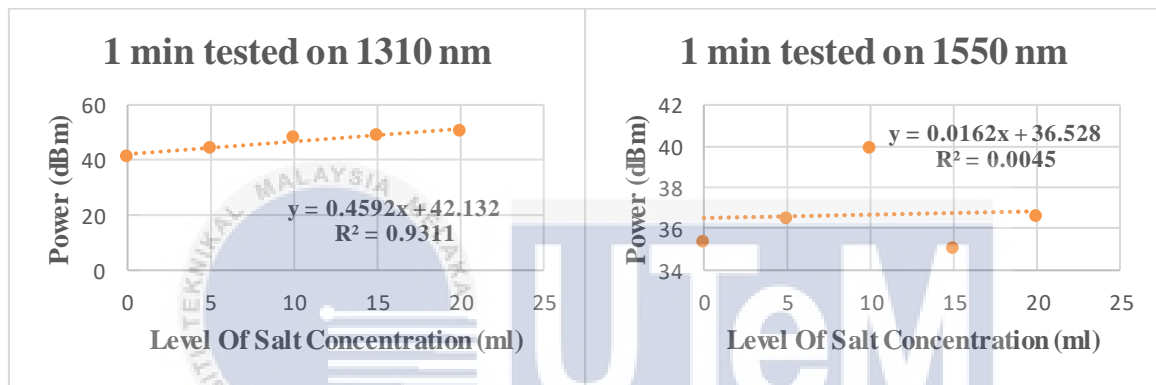


Figure 4.12 Microfiber optic single loop sensor response at 1 minutes

Table 4.13 presents data recorded in the first minute of the conducted experiment for both 1310nm and 1550nm optical light sources, showcasing varying levels of salt concentration and the differences between these two wavelengths. For the 1310nm optical light wavelength, the output power (dBm) reading increases from 41.36 dBm at 0ml salt concentration to 50.471 dBm at 20ml salt concentration. Conversely, for the 1550nm wavelength, there is an increase in the output power (dBm) from 35.43 dBm at 0ml salt concentration to 36.57 dBm at 20ml salt concentration. Figure 4.12 illustrates the gradient values at both wavelengths across different levels of concentration. In the initial minute, the 1310nm wavelength recorded the highest gradient at 0.4592, while the gradient for the 1550nm wavelength was only 0.0162.

#### 4.6.1.2 2 Minutes Tested on 1310nm and 1550nm Wavelength.

Table 4.14 Recorded data for 2 minutes

Output Power of 2 minutes (dBm)		
Level of salt concentration (ml)	1310nm	1550nm
0	43.87	36.57
5	46.56	39.11
10	48.61	40.7
15	50	36.29
20	50.58	36.57

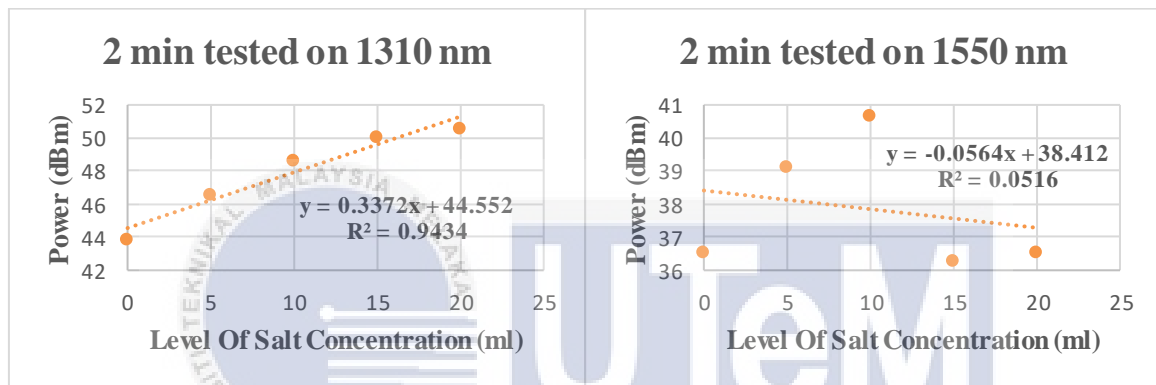


Figure 4.13 Microfiber optic single loop sensor response at 2 minutes

Table 4.14 presents the data recorded for the output power value (dBm) at the 2nd minute for both optical light sources with different wavelengths. This data reveals a decrease in output power (dBm) from 43.87 dBm at 0ml salt concentration to 50.58 dBm at 20ml salt concentration for the 1310nm optical light source. In contrast, the 1550nm wavelength starts at 36.57 dBm at 0ml salt concentration and remains at 36.57 dBm at 20ml salt concentration. Figure 4.13 illustrates the gradient difference between the two optical light sources with different wavelengths. In the second minute, the 1310nm wavelength proves more sensitive than the 1550nm wavelength due to the higher gradient value, measuring 0.3372 compared to the 1550nm wavelength's -0.0564.

#### 4.6.1.3 3 Minutes Tested on 1310nm and 1550nm Wavelength.

Table 4.15 Recorded data for 3 minutes

Output Power of 3 minutes (dBm)		
Level of salt concentration (ml)	1310nm	1550nm
0	44.54	36.73
5	46.88	39.59
10	48.99	40.9
15	50.24	36.45
20	51.37	36.82

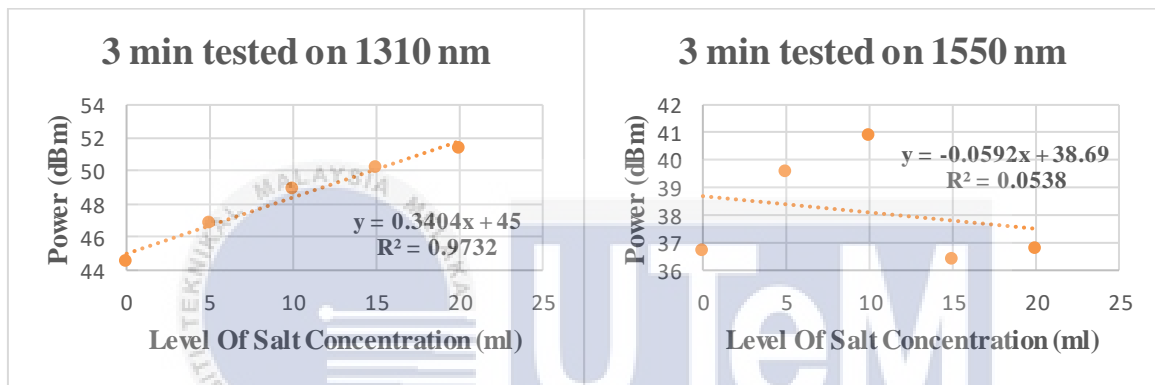


Figure 4.14 Microfiber optic single loop sensor response at 3 minutes

Table 4.15 displays the power output (dBm) values recorded at the 3rd minute for various levels of salt concentration for both wavelengths. There is an increase observed from the 0ml level of salt concentration to the 20ml level for both wavelengths. However, the increase at the 1310 nm wavelength is more substantial, measuring 6.83 dBm, compared to the 1550 nm wavelength, which registers a modest increase of 0.09 dBm from 0ml to 20ml salt concentration. Figure 4.14 visually represents the sensor's response to salt concentration in the 3rd minute. From this diagram, it can be concluded that, in the 3rd minute, the 1310nm wavelength is more responsive to concentration, exhibiting a gradient of 0.3404, while the 1550nm wavelength shows a lower gradient of -0.0592.

#### 4.6.1.4 4 Minutes Tested on 1310nm and 1550nm Wavelength.

Table 4.16 Recorded data for 4 minutes

Output Power of 4 minutes (dBm)		
Level of salt concentration (ml)	1310nm	1550nm
0	45.02	36.75
5	46.98	40.01
10	49.1	40.95
15	50.89	36.48
20	51.69	36.82

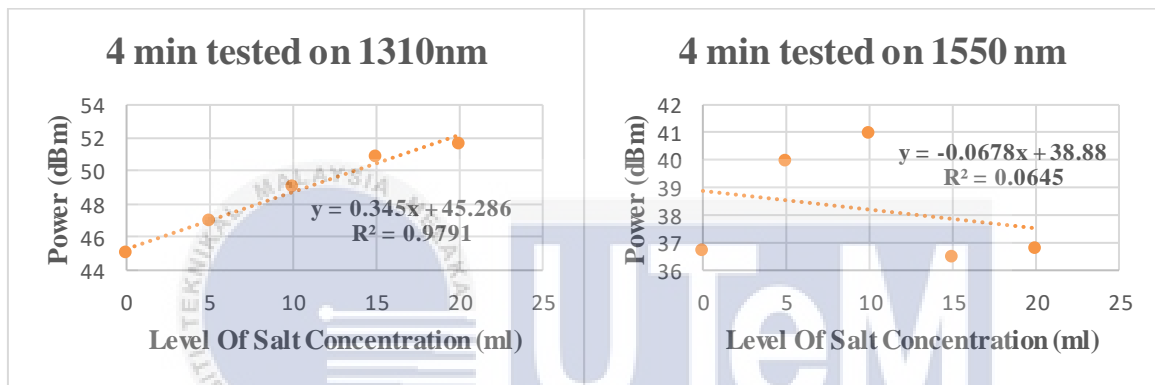


Figure 4.15 Microfiber optic single loop sensor response at 4 minutes

The output power (dBm) values for each level of salt concentration for both wavelengths at the fourth minute are presented in Table 4.16. The concentration for these two wavelengths increases from 0ml to 20ml. However, the elevation from 0ml to 20 ml salt concentration at the 1310 nm wavelength is more substantial (6.67 dBm) than at the 1550 nm wavelength (0.07 dBm). The sensor's response to concentration during the fourth minute is depicted in Figure 4.15. This diagram illustrates that in the fourth minute, the gradient at the 1550nm wavelength is more significant at -0.0678, whereas at the 1310nm wavelength, it is 0.345, indicating greater responsiveness to concentrations.

#### 4.6.1.5 5 Minutes Tested on 1310nm and 1550nm Wavelength.

Table 4.17 Recorded data for 5 minutes

Output Power of 5 minutes (dBm)		
Level of salt concentration (ml)	1310nm	1550nm
0	45.13	36.77
5	47.26	40.13
10	49.29	40.96
15	51.08	36.5
20	52.4	36.86

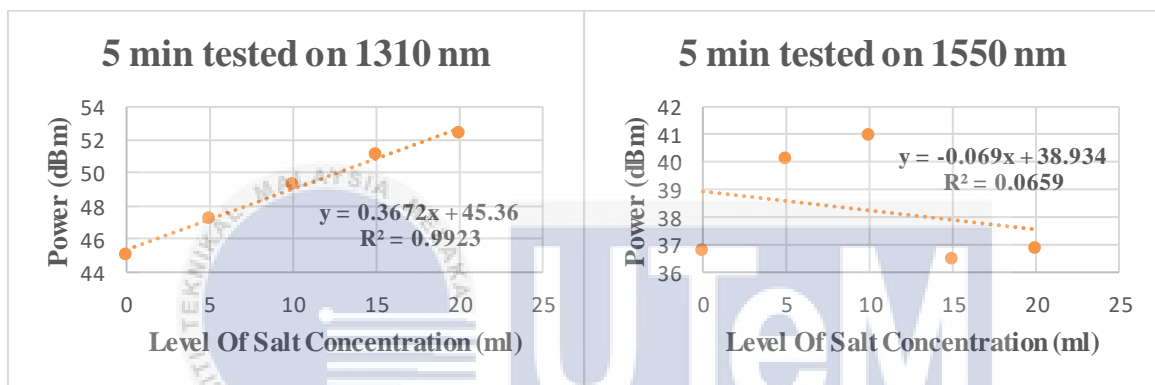


Figure 4.16 Microfiber optic single loop sensor response at 5 minutes

The recorded output power (dBm) values for each distinct salt concentration level at the fifth minute are presented in Table 4.17. The concentration for both wavelengths increases from 0ml to 20ml. Notably, the elevation from 0ml to 20ml salt concentration at the 1310 nm wavelength is more pronounced (7.27 dBm) compared to the 1550 nm wavelength (0.09 dBm). The sensor's response to concentration during the fifth minute is illustrated in Figure 4.16. This diagram indicates that in the fifth minute, the gradient at the 1550nm wavelength is more notable at -0.069, whereas at the 1310nm wavelength, it is 0.3672, highlighting a higher sensitivity to concentration.

#### 4.6.1.6 6 Minutes Tested on 1310nm and 1550nm Wavelength.

Table 4.18 Recorded data for 6 minutes

Output Power of 6 minutes (dBm)		
Level of salt concentration (ml)	1310nm	1550nm
0	45.19	36.77
5	47.35	40.14
10	49.62	41.01
15	51.24	36.5
20	55.13	36.88

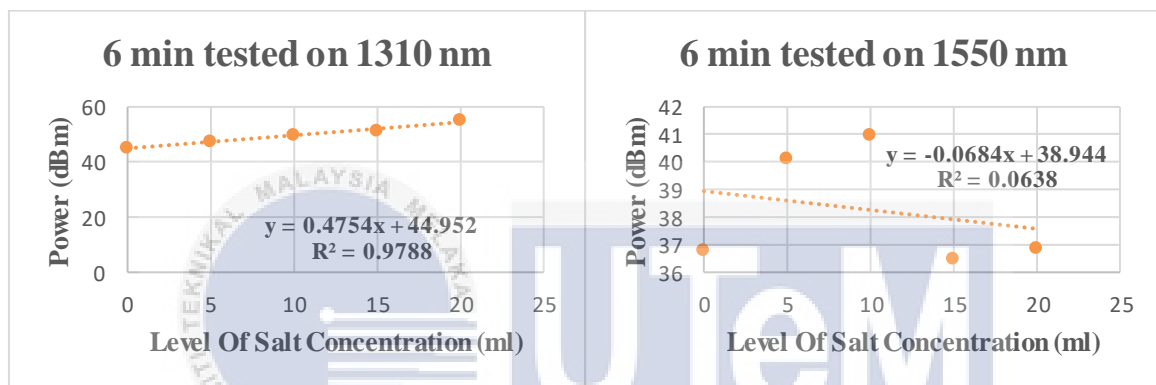


Figure 4.17 Microfiber optic single loop sensor response at 6 minutes

Table 4.18 displays the output power (dBm) values for each level of salt concentration at the sixth minute for both wavelengths. The relative concentration increases from 0ml to 20ml for these two wavelengths. However, the disparity between 0ml to 20ml relative concentration is more pronounced at the 1310 nm wavelength, measuring 9.94 dBm, compared to the 1550 nm wavelength (0.11 dBm). Figure 4.17 illustrates the sensor's response to concentration during the sixth minute. This graph shows that in the sixth minute, the gradient at 1550 nm is -0.0684, while it is 0.4754 at 1310 nm, indicating that the 1310 nm wavelength is more responsive to concentration.

**4.6.1.7.7 Minutes Tested on 1310nm and 1550nm Wavelength.**

Table 4.19 Recorded data for 7 minutes

Output Power of 7 minutes (dBm)		
Level of salt concentration (ml)	1310nm	1550nm
0	45.31	36.78
5	47.42	40.19
10	50.05	41.06
15	51.31	36.5
20	55.76	36.88

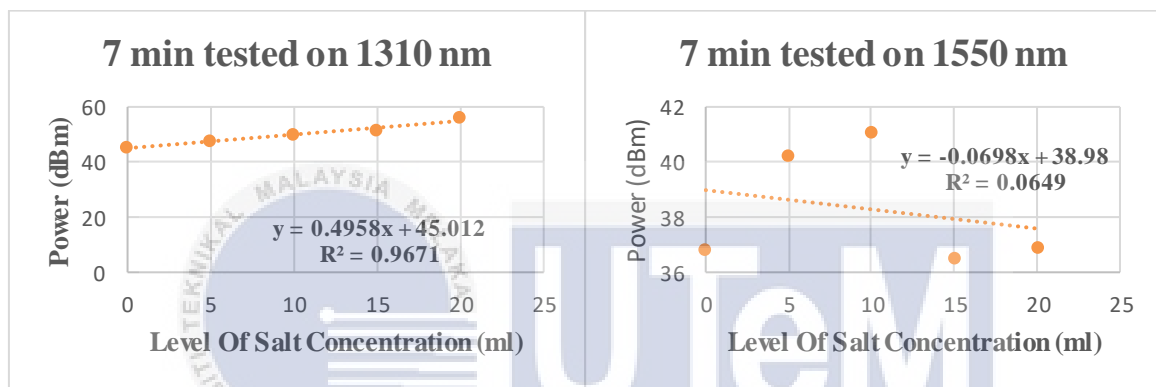


Figure 4.18 Microfiber optic single loop sensor response at 7 minutes

Table 4.19 presents the output power (dBm) values for both wavelengths at 7 minutes for each distinct level of salt concentration, ranging from 0ml to 20ml. Notably, there is a decrease in output power at the 1310 nm wavelength by 10.45 dBm, whereas, conversely, at the 1550 nm wavelength, the reduction in concentration from 0ml to 20ml is smaller, measuring only 0.1 dBm. Figure 4.18 illustrates the sensor's response to concentration at that specific time. The graph indicates that the gradient at the 1310nm wavelength is more sensitive to concentration, with a value of 0.4958, compared to the 1550nm wavelength, which exhibits a gradient at 7 minutes of -0.0698.

#### 4.6.2 Result for Double Loop

This part shows the data recorded by using 0ml, 5ml, 10ml, 15ml and 20ml level of salt concentration on 1310nm and 1550nm from 1 minutes to 7 minutes in a single loop resonator.

##### 4.6.2.1 1 Minutes Tested on 1310nm and 1550nm Wavelength.

Table 4.20 Recorded data for 1 minutes

Output Power of 1 minutes (dBm)		
Level of salt concentration (ml)	1310nm	1550nm
0	41.94	37.68
5	44.18	38.77
10	43.52	39.7
15	40.87	38.46
20	41.4	38.89

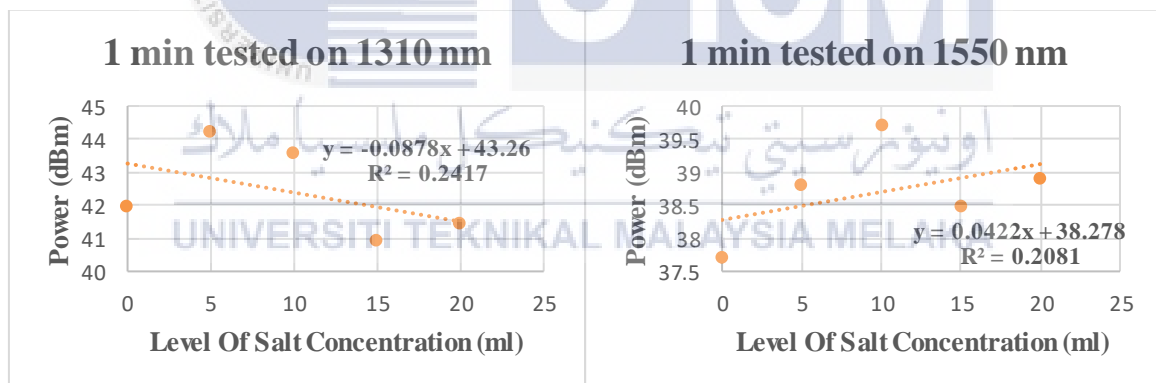


Figure 4.19 Microfiber optic double loop sensor response at 1 minutes

Table 4.20 displays the data recorded in the initial minute of this experiment for both 1310nm and 1550nm optical light sources, varying across different salt concentration levels and showcasing the differences between these wavelengths. In the case of the 1310nm optical light wavelength, the output power (dBm) reading decreases from 41.94 dBm at 0ml salt concentration to 41.4 dBm at 20ml salt concentration. Conversely, for the 1550nm

wavelength, there is an increase in the output power (dBm) from 37.68 dBm at 0ml salt concentration to 38.89 dBm at 20ml salt concentration. Figure 4.19 depicts the gradient values at both wavelengths with varying levels of concentration. During the initial minute, the 1310nm wavelength recorded the least gradient of -0.0878, while the gradient for the 1550nm wavelength was only 0.0422.

#### 4.6.2.2 2 Minutes Tested on 1310nm and 1550nm Wavelength.

Table 4.21 Recorded data for 2 minutes

Output Power of 2 minutes (dBm)		
Level of salt concentration (ml)	1310nm	1550nm
0	42.77	38.82
5	45.01	39.08
10	45.04	39.86
15	42.54	39.43
20	43.26	39.48

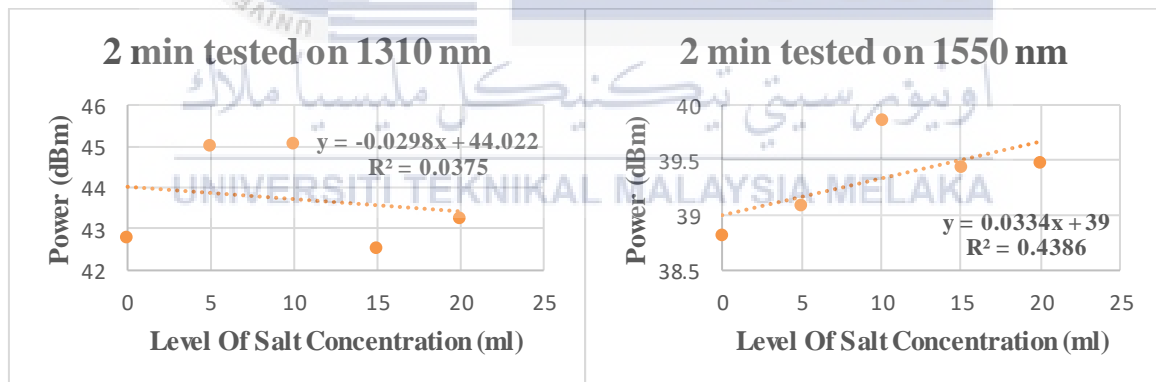


Figure 4.20 Microfiber optic double loop sensor response at 2 minutes

Table 4.21 presents the data recorded for the output power values (dBm) at the 2nd minute for both optical light sources with different wavelengths. This data indicates an increase in output power (dBm) from 42.77 dBm at 0ml salt concentration to 43.26 dBm at 20ml salt concentration for the 1310nm optical light source. In contrast, the 1550nm wavelength starts at 38.82 dBm at 0ml salt concentration and reaches 39.48 dBm at 20ml

salt concentration. Figure 4.20 illustrates the gradient difference between the two optical light sources. During the second minute, the 1550nm wavelength proves more sensitive than 1310nm due to the higher gradient value of 0.0334, compared to the 1310nm wavelength's -0.0298.

**4.6.2.3 3 Minutes Tested on 1310nm and 1550nm Wavelength.**

Table 4.22 Recorded data for 3 minutes

Output Power of 3 minutes (dBm)		
Level of salt concentration (ml)	1310nm	1550nm
0	43.66	40.11
5	45.18	40.18
10	45.43	39.98
15	42.89	40.33
20	43.41	39.87

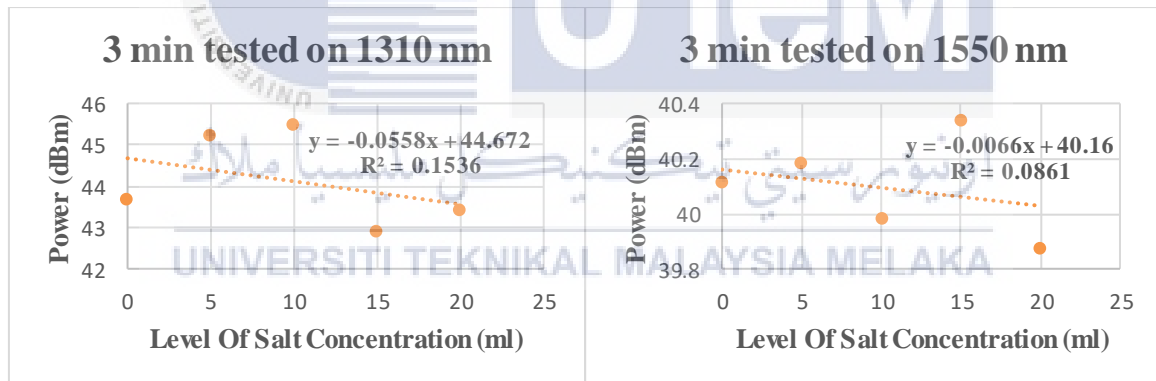


Figure 4.21 Microfiber optic double loop sensor response at 3 minutes

Table 4.22 displays the recorded power output values (dBm) at the 3rd minute for various levels of salt concentration for both wavelengths. There is a decline observed from 0ml to 20ml salt concentration for both wavelengths. However, the decrease at the 1310nm wavelength is greater, measuring 0.25 dBm, compared to the 1550nm wavelength, which experiences a decrease of 0.24 dBm from 0ml to 20ml salt concentration. Figure 4.21

illustrates the sensor's response to salt concentration in the 3rd minute. From this diagram, it can be inferred that, in the 3rd minute, the 1550nm wavelength exhibits greater responsiveness to concentration with a gradient of -0.0066, while at the 1310nm wavelength, the gradient is -0.0558.

#### 4.6.2.4 4 Minutes Tested on 1310nm and 1550nm Wavelength.

Table 4.23 Recorded data for 4 minutes

Output Power of 4 minutes (dBm)		
Level of salt concentration (ml)	1310nm	1550nm
0	43.89	40.41
5	45.26	40.24
10	45.49	40.01
15	43.12	40.49
20	43.5	40

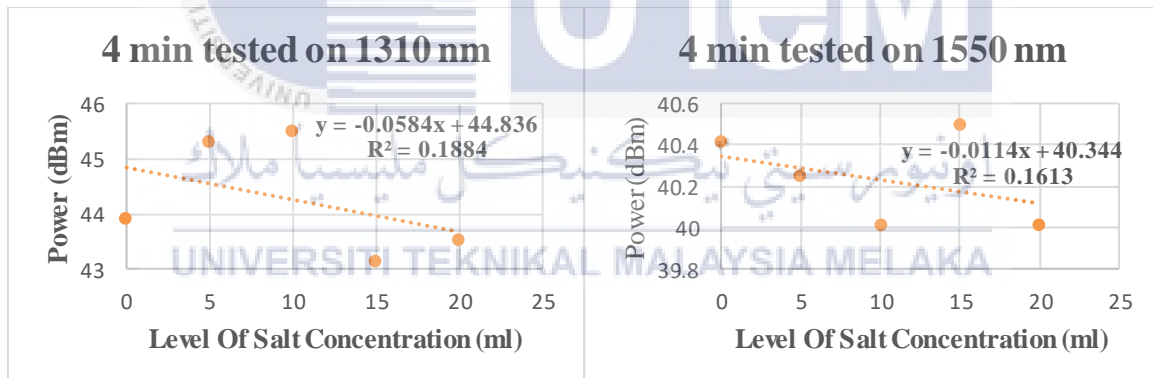


Figure 4.22 Microfiber optic double loop sensor response at 4 minutes

The output power values (dBm) for various levels of salt concentration for both wavelengths at the fourth minute are presented in Table 4.23. The concentration for these two wavelengths decreases from 0ml to 20ml. However, the decline from 0ml to 20ml salt concentration at the 1550nm wavelength is 0.39 dBm than at the 1310nm wavelength (0.41 dBm). The sensor's response to concentration during the fourth minute is illustrated in Figure 4.22. This diagram reveals that in the fourth minute, the gradient at the 1310nm wavelength

is more significant at -0.0584, while it is -0.0114 at the 1550nm wavelength, indicating greater responsiveness to concentration.

**4.6.2.5 5 Minutes Tested on 1310nm and 1550nm Wavelength.**

Table 4.24 Recorded data for 5 minutes

Output Power of 5 minutes (dBm)		
Level of salt concentration (ml)	1310nm	1550nm
0	44.26	40.5
5	45.36	40.32
10	45.53	40.07
15	43.17	40.56
20	43.56	40.02

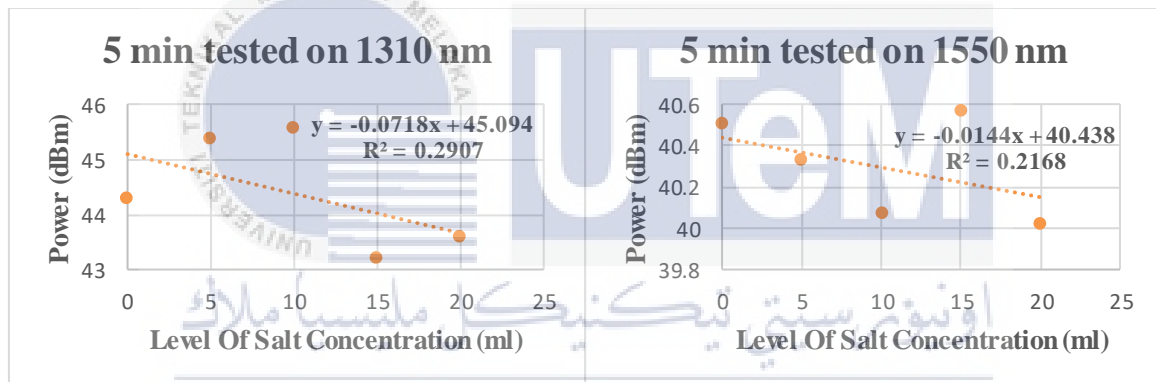


Figure 4.23 Microfiber optic double loop sensor response at 5 minutes

The recorded output power values (dBm) for various levels of salt concentration for both wavelengths at the fifth minute are displayed in Table 4.24. The concentration for these two wavelengths decreases from 0ml to 20ml. However, the decline from 0ml to 20ml salt concentration at the 1310nm wavelength is more substantial (0.7 dBm) than at the 1550nm wavelength (0.48 dBm). The sensor's response to concentration during the fifth minute is illustrated in Figure 4.23. This diagram reveals that in the fifth minute, the gradient at the 1310nm wavelength is more significant at -0.0718, while it is -0.0144 at the 1550nm wavelength, indicating higher responsiveness to concentrations.

#### 4.6.2.6 6 Minutes Tested on 1310nm and 1550nm Wavelength.

Table 4.25 Recorded data for 6 minutes

Output Power of 6 minutes (dBm)		
Level of salt concentration (ml)	1310nm	1550nm
0	44.98	40.52
5	45.89	40.33
10	45.63	40.08
15	43.19	40.63
20	43.56	40.07

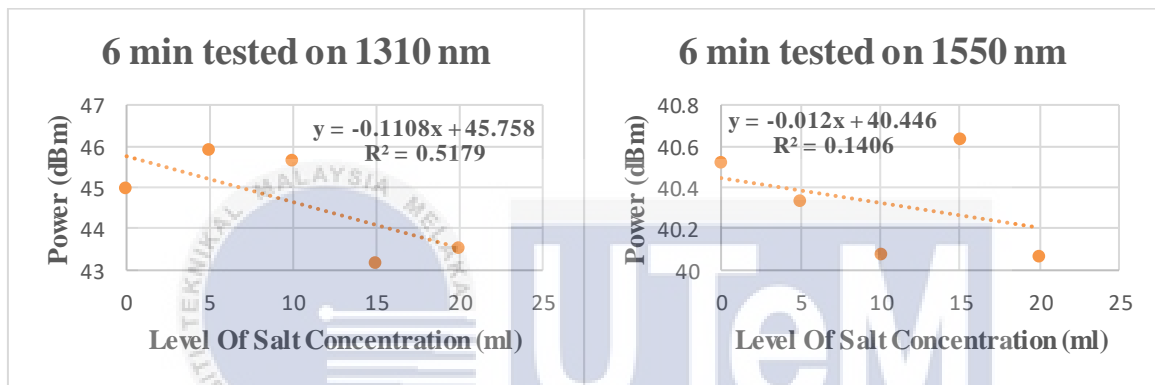


Figure 4.24 Microfiber optic double loop sensor response at 6 minutes

Table 4.25 displays the output power (dBm) values for each level of salt concentration at the sixth minute for both wavelengths. The relative concentration increases from 0ml to 20ml for these two wavelengths. However, the difference in relative concentration from 0ml to 20ml is more pronounced at the 1310 nm wavelength, measuring 1.42 dBm, compared to the 1550 nm wavelength (0.43 dBm). Figure 4.24 illustrates the sensor's response to concentration during the sixth minute. This graph indicates that in the sixth minute, the gradient at 1310 nm is -0.1108, while it is -0.012 at 1550 nm, suggesting that the 1550 nm wavelength is more responsive to concentration.

**4.6.2.7 7 Minutes Tested on 1310nm and 1550nm Wavelength.**

Table 4.26 Recorded data for 7 minutes

Output Power of 7 minutes (dBm)		
Level of salt concentration (ml)	1310nm	1550nm
0	45.56	40.53
5	46.2	40.38
10	45.63	40.1
15	43.24	40.69
20	43.57	40.11

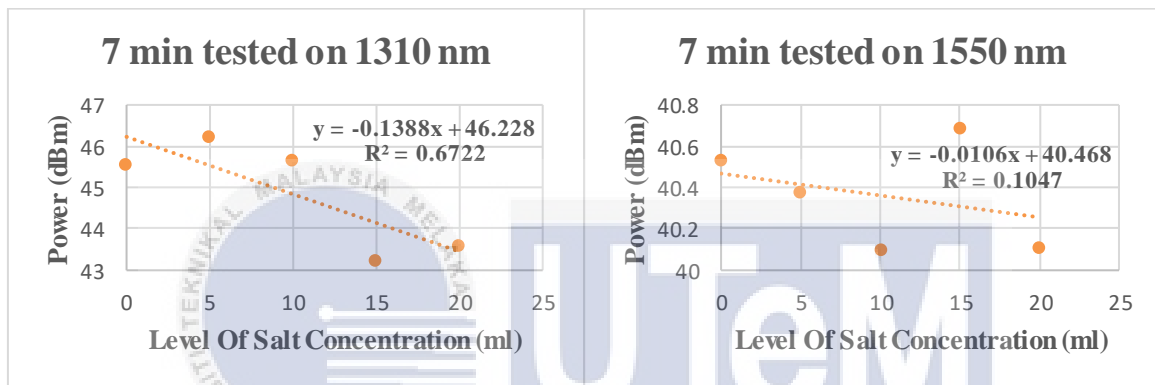


Figure 4.25 Microfiber optic double loop sensor response at 7 minutes

Table 4.26 presents the output power values (dBm) for both wavelengths at 7 minutes for each specific level of salt concentration. The values increase from 0ml to 20ml for both wavelengths. However, there is a decrease at the 1310 nm wavelength of 1.99 dBm, while conversely, at the 1550 nm wavelength, the reduction in concentration from 0ml to 20ml is smaller, measuring at 0.42 dBm. The sensor's reaction to the concentration at that time is depicted in Figure 4.25. The graph reveals that the gradient at the 1550nm wavelength is more responsive to concentration compared to the gradient at the 1310nm wavelength, showing values at 7 minutes of -0.0106 versus -0.1388.

### 4.6.3 Comparison between 1310nm and 1550nm for Single Loop

Table 4.27 Recorded data for output power (dBm) at 1310nm and 1550nm optical light source with different time (m).

Time (m)	1310nm		1550nm	
	Sensitivity (dBm)	Linearity (%)	Sensitivity (dBm)	Linearity (%)
1	0.4592	96.49	0.0162	6.71
2	0.3372	97.13	-0.0564	22.72
3	0.3404	98.65	-0.0592	23.19
4	0.345	98.95	-0.0678	25.40
5	0.3672	99.61	-0.069	25.67
6	0.4754	98.93	-0.0684	25.26
7	0.4958	98.34	-0.0698	26.38

Table 4.27 presents the recorded data for both optical light sources, namely 1310 nm and 1550 nm, highlighting the variations over time. These values are gathered to assess the microfiber loop sensor's reaction to changes in salt concentration over time. The findings suggest that at the 1310 nm optical light source wavelength, there is greater responsiveness to concentration in the 7th minute, as evidenced by the highest recorded value of 0.4958. In contrast, the 1550 nm wavelength displays effective interaction during the initial minute of the sensing process, recording the highest value of 0.0162, setting it apart from subsequent measurements at the same wavelength.

#### 4.6.4 Comparison between 1310nm and 1550nm for Double Loop

Table 4.28 Recorded data for output power (dBm) at 1310nm and 1550nm optical light source with different time (m).

Time (m)	1310nm		1550nm	
	Sensitivity (dBm)	Linearity (%)	Sensitivity (dBm)	Linearity (%)
1	-0.0878	49.16	0.0422	45.62
2	-0.0298	19.36	0.0334	66.22
3	-0.0558	39.19	-0.0066	29.34
4	-0.0584	43.41	-0.0114	40.16
5	-0.0718	53.92	-0.0144	46.56
6	-0.1108	71.97	-0.012	37.49
7	-0.1388	81.99	-0.0106	32.36

Table 4.28 presents recorded data for both optical light sources, specifically at 1310 nm and 1550 nm, indicating the differences observed at each time point. These values are collected to assess the microfiber double-loop sensor's response to changes in salt concentration over time. It can be concluded that at the wavelength of 1310 nm optical light source, there is greater ease of interaction with concentration in the 2nd minute, as indicated by the highest recorded value of -0.0298. In contrast, at the 1550 nm wavelength, effective interaction occurs during the 2nd minute of the sensing process, with the highest value of 0.0334, setting it apart from others at the same wavelength.

#### 4.6.5 Average 1310nm and 1550nm for Single Loop

Table 4.29 Recorded data for average output power (dBm)

Average output power (dBm)		
Level of salt concentration (ml)	1310nm	1550nm
0	44.35	36.54
5	46.69	39.38
10	49.14	40.78
15	50.55	36.25
20	52.49	36.77

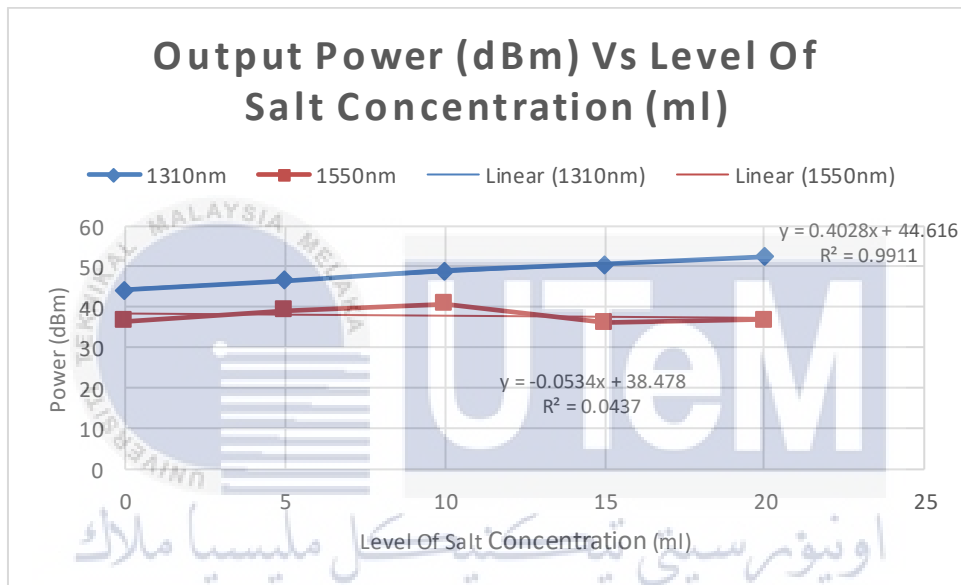


Figure 4.26 Fiber optic sensor response at both of wavelength

In this comparison section, the average output power value (dBm) pads a Table 4.29 for wavelength 1310 nm and 1550 nm optical light source for each level of salt concentration has been recorded to make a comparison and determine between these two wavelengths, which one is more sensitive. Based on Figure 4.26 shows both optical light source gradients. To make a microfiber loop sensor for liquid, a wavelength 1310 nm optical light source is the most suitable because it is more sensitive to liquid. This can be proven by the gradient value obtained, which is 0.4028, compared to the wavelength of 1550 nm optical light source, which is -0.0534.

#### 4.6.6 Average 1310nm and 1550nm for Double Loop

Table 4.30 Recorded data for average output power (dBm)

Average output power (dBm)		
Level of salt concentration (ml)	1310nm	1550nm
0	43.87	39.80
5	45.30	39.9
10	45.18	39.97
15	42.71	40.08
20	43.18	39.78

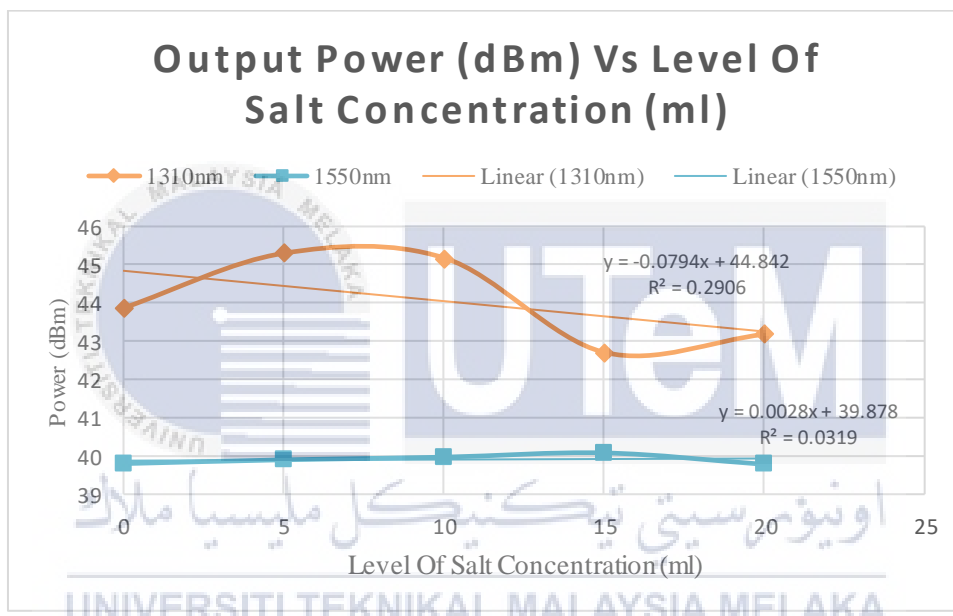


Figure 4.27 Fiber optic sensor response at both of wavelength

In this comparison section, the average output power value (dBm) pads a Table 4.30 for wavelength 1310 nm and 1550 nm optical light source for each level of salt concentration has been recorded to make a comparison and determine between these two wavelengths, which one is more sensitive. Based on Figure 4.27 shows both optical light source gradients. To make a microfiber loop sensor for liquid, a wavelength 1550 nm optical light source is the most suitable because it is more sensitive to liquid. This can be proven by the gradient value obtained, which is 0.0028, compared to the wavelength of 1310 nm optical light source, which is -0.0794.

## CHAPTER 5

### CONCLUSION AND RECOMMENDATIONS

#### 5.1 Conclusion

This chapter provides a summary of the Microfiber Double Loop Resonator for Liquid Sensor in used for medical industry. The project builds upon prior research and literature reviews from various studies focusing on optical fiber as a sensor in the medical sector. Creating a sensor tailored for the medical industry is crucial, given the need for precise equipment to save lives. The project's methodology includes the application of tools such as stripping, cleaving, and splicing the optical fiber cable, specifically chosen to suit liquid sensing applications. All these methods are meticulously implemented to bring the project to fruition.

This project involves testing with varying levels of salt concentration using different looping configurations, such as single loop and double loop. The results compare the effectiveness of each loop under different salt concentrations.

The project's findings indicate that the relative liquid levels can be determined with liquid sensors connected to optical fiber, as the experiment detects subtle changes in the liquid levels. However, for this to evolve into a successful fiber optic sensor project for the medical industry, the construction of a liquid sensor based on optical microfiber loops still requires significant development and improvement.

## 5.2 Future Works

This research has shown that the Microfiber Double Loop Resonator works well as a liquid sensor. However, there are many exciting possibilities for future research that could make it even better and useful in more ways. The ideas below suggest different ways we could explore in future studies:

- i) By exploring another wavelength. This could potentially optimize the sensor's performance.
- ii) Testing the sensor with different types of liquids or varying concentrations of other solutes. This could broaden the applicability of the sensor in different scenarios in the medical field.
- iii) Comparing the Microfiber Double Loop Resonator with other resonator designs. This could provide insights into which design is most effective for specific applications.
- iv) Investigate how environmental factors such as temperature and humidity affect the sensor's performance. This could be important for real-world applications where conditions can vary.
- v) Based on the sensitivity values obtained at different concentrations and wavelengths, a standard calibration procedure can be developed for these sensors. This would help in achieving more accurate and reliable measurements in practical applications.

## REFERENCES

- [1] S. Addanki, I. S. Amiri, and P. Yupapin, "Review of optical fibers-introduction and applications in fiber lasers," *Results Phys*, vol. 10, 2018, doi: 10.1016/j.rinp.2018.07.028.
- [2] I. Floris, J. M. Adam, P. A. Calderón, and S. Sales, "Fiber Optic Shape Sensors: A comprehensive review," *Optics and Lasers in Engineering*, vol. 139. 2021. doi: 10.1016/j.optlaseng.2020.106508.
- [3] V. G. M. Annamdas, "Review on Developments in Fiber Optical Sensors and Applications," *International Journal of Materials Engineering*, vol. 1, no. 1, 2012, doi: 10.5923/j.ijme.20110101.01.
- [4] R. Imani and G. Huerta Cuellar, "Introductory Chapter: Optical Fibers," in *Optical Fiber Applications*, 2020. doi: 10.5772/intechopen.91397.
- [5] M. Rekha, M. Singh, and B. Raj, "SINGLE MODE FIBER STANDARDS: A REVIEW."
- [6] M. J. Li and D. A. Nolan, "Optical transmission fiber design evolution," *Journal of Lightwave Technology*, vol. 26, no. 9. 2008. doi: 10.1109/JLT.2008.922150.
- [7] A. Rovera, A. Tancau, N. Boetti, M. D. L. Dalla Vedova, P. Maggiore, and D. Janner, "Fiber Optic Sensors for Harsh and High Radiation Environments in Aerospace Applications," *Sensors*, vol. 23, no. 5. 2023. doi: 10.3390/s23052512.
- [8] R. Correia, S. James, S. W. Lee, S. P. Morgan, and S. Korposh, "Biomedical application of optical fibre sensors," *Journal of Optics (United Kingdom)*, vol. 20, no. 7. 2018. doi: 10.1088/2040-8986/aac68d.
- [9] L. Xie, R. Li, B. Zhang, J. Wang, and C. Zhang, "Influence of single mode fiber bending on fiber optic gyroscopescale factor stability," *Hongwai yu Jiguang*

- Gongcheng/Infrared and Laser Engineering*, vol. 45, no. 1, 2016, doi: 10.3788/IRLA201645.0122001.
- [10] Y. H. Kim, K. S. Park, B. H. Lee, S. Lee, D. H. Woo, and Y. T. Chough, “Highly accurate refractive index sensor based on fourier-transformed phase acquisition in fiber-optic interferometer,” in *Proceedings of the International Conference on Sensing Technology, ICST*, 2013. doi: 10.1109/ICSensT.2013.6727714.
- [11] S. Korposh, S. W. James, S. W. Lee, and R. P. Tatam, “Tapered Optical Fibre Sensors: Current Trends and Future Perspectives,” *Sensors (Basel, Switzerland)*, vol. 19, no. 10. 2019. doi: 10.3390/s19102294.
- [12] C. Liu *et al.*, “Sagnac interferometer-based optical fiber strain sensor with exceeding free spectral measurement range and high sensitivity,” *Opt Laser Technol*, vol. 159, 2023, doi: 10.1016/j.optlastec.2022.108935.
- [13] K. N. Koo *et al.*, “Tailoring surface structure and diameter of etched fiber Bragg grating for high strain sensing,” *Opt Laser Technol*, vol. 157, 2023, doi: 10.1016/j.optlastec.2022.108693.
- [14] S. Zoriatatin and E. Arzi, “A multi-purpose reflective fiber optic sensor,” *J Mod Opt*, vol. 60, pp. 781–789, Jun. 2013.

## APPENDICES

### Appendix A Gantt Chart for PSM 1

PROJECT ACTIVITY/TASK	WEEK													
	1	2	3	4	5	6	7	8	9	10	11	12	13	14
Project Briefing	X													
Research Project	X													
Background, Problem statement & Objective		X	X											
Identify component			X											
Make project proposal			X	X	X									
Project flow chart					X									
Methodology					X		X							
Review report								X	X	X				
Submit 1st draft report											X			
Submit report												X	X	
Presentation														X